THE CATHOLIC UNIVERSITY OF AMERICA

Genetic and Biochemical Characterization of the Signaling Interface and the Deviant ATP Binding Site in the Yeast Multidrug Transporter Pdr5

A DISSERTATION

Submitted to the Faculty of the

Department of Biology

School of Art and Sciences

Of The Catholic University of America

In Partial Fulfillment of the Requirements

For the Degree

Doctor of Philosophy

By

Neeti Ananthaswamy

Washington, D.C.

2012

Genetic and Biochemical Characterization of the Signaling Interface and the Deviant ATP Binding Site in the Yeast Multidrug Transporter Pdr5

Neeti Ananthaswamy, Ph.D.

John E. Golin, Ph.D

Pdr5 is an ABC transporter in *Saccharomyces cerevisiae* that facilitates xenobiotic efflux. Like all ABC transporters Pdr5 is composed of a pair of transmembrane domain (TMDs) that contain substrate binding pockets and a pair of nucleotide binding domains (NBDs) that power substrate transport. The NBD contains conserved motifs including Walker A, Walker B, Q-loop and Signature that facilitate ATP binding/hydrolysis. At each ATP binding site, an ATP molecule is sandwiched between Walker A, Walker B, Q-loop of one NBD and Signature of the other. In the Pdr family of fungal transporters, one of the ATP binding sites is canonical, known to bind/hydrolyze ATP. The other ATP binding site, however, is made up deviant residues.

Hydrolysis of ATP at the NBD is thought to cause a conformational change at the TMDs. X-ray structure of Sav1866 implicates Q-loop and the intercellular loops in communication between the TMDs and the NBDs. In order to determine the signal interface in Pdr5, we evaluated the role of the Q loop residues, E244 in NBD1 and Q951 in NBD2. Surprisingly, mutation of these conserved residues exhibited only mild drug hyper sensitivity and retained significant ATPase activity. The double mutant showed a greater than additive sensitivity, indicating a functional overlap between the two Q loops. Interestingly, the reduced ATPase activity of the double mutant was equal

to the single mutants. It is likely, therefore that the Q-loop residues are involved in interdomain communication.

The precise function of the deviant ATP site in Pdr5 remains unclear. In order to elucidate its role, we evaluated the contribution of the deviant Walker A (C199) and a residue in the deviant signature motif (E1013). Mutating these residues to alanine exhibited only moderate drug hypersensitivity. They also retained significant ATPase activity, indicating that the deviant Walker A and Signature are not catalytic. As expected, mutating K911 in Walker A and G312 in the signature of the canonical site creates a null phenotype. This indicates that the deviant and the canonical ATP binding sites are not equivalent. We propose that the deviant site might regulate ATP hydrolysis at the canonical site.

This dissertation by Neeti Ananthaswamy fulfills the dissertation requirement for the doctoral degree in the Department of Biology approved by John E. Golin, PhD., as Director, and by Venigalla B. Rao, Ph.D., Pamela L. Tuma, Ph.D., and Ann K. Corsi, Ph.D., as Readers.

_____
John E. Golin, PhD., Director

_____
Venigalla B. Rao, Ph.D., Reader

_____
Pamela L. Tuma, Ph.D., Reader

_____
Ann K. Corsi, Ph.D., Reader

TABEL OF CONTENTS

List of Illustrations vi

List of Tables vii

Abbreviations viii

Introduction 1

Structure of ABC transporters 1
- Transmembrane Domains 2
- Nucleotide Binding Domains 2

Energetics of transport 3
- Step I: Ligand binding to the TMDs 4
- Step II: Closed dimer formation – power stroke for transport 4
- Step III: ATP hydrolysis 5
- Step IV: Release of P_i and ADP 5

Asymmetric ABC transporters 6
- Cystic fibrosis transmembrane conductance regulator 6
- Transporter associated with antigen processing 8
- LmrCD 9

Phylognetic classification of ABC transporters 10
- ABC-A (Subfamily A) 10
- ABC-B (Subfamily B) 11
- ABC-C (Subfamily C) 12
- ABC-D (Subfamily D) 12
- ABC-E and ABC-F (Subfamily E and F) 13
- ABC-G (Subfamily G) 13

ABC transporters in yeast 14
- ABC transporters in *Saccharomyces cerevisiae* 14

Molecular modeling of Pdr5 15
- Modeling of transmembrane helices (TMH's) 16
- Modeling of the nucleotide binding domains (NBD's) 17

Defining a Signal Interface in ABC Transporters 20

Materials and Methods 23
Strains, Plasmid, Media and Drugs 23
Primers 24
Sequencing of PDR5 gene 24
Electrophoresis 25
Agarose gel electrophoresis 25
Protein gel electrophoresis 26
Polymerase Chain Reaction 26
Site Directed Mutagenesis of PDR5 in pSS607 26
Amplification of PDR5 from yeast chromosomal DNA 28
Preparation of DNA 29
Purification of plasmid DNA from *E.coli* 29
Extraction of yeast genomic DNA 30
Transformation Techniques 31
Bacterial transformation 31
Transformantion of plasmid DNA into yeast 33
5FOA testing and selection on G-418 34
Drug Sensitivity Testing 34
Spot test 34
IC-50 in liquid culture 35
Rhodamine 6G transport assay 35
Plasma Membrane Isolation and Quantification 36
Isolation of yeast plasma membrane 36
Plasma membrane protein quantification 38
Western Blotting 38
Plasma Membrane Analysis 39
ATPase assay 39
Isolation of Second-site Suppressor Mutation in PDR5 40

Results 43

PART I: Mapping the signaling interface in Pdr5 43

Isolation and sequence analysis of mutants that suppress the clotrimazole hypersensitivity of S558Y 43
The drug phenotypes of the suppressor mutants 48
The effect of NBD mutations in a S558 (otherwise WT) background 50
Double-mutant analysis: redundancy of Q-loop function during ATP hydrolysis 52
The effect of Q-region mutations on NTPase activity 54

PART II: Deviant ATP Binding Site of Pdr5: Evidence for a Novel Functional Role 59

The deviant signature motif residue Glu-1013 is not equivalent to its canonical counterpart Gly-312 59
Drug phenotype of C199A is very similar to E1013A 62
E1013A and C199A retains significant ATPase activity 63
The suppressors of E1013A lie outside PDR5 65
SUP5 and SUP6 localize in membrane at levels equivalent to WT 69
The suppressor phenotype requires Pdr5 protein 70
SUP5 restores ATPase activity to WT levels 71
Microarray analysis of SUP5 72

Discussion 75

References 87

LIST OF ILLUSTRATIONS

Figure 1	Experimental strategy to determine whether a reversion phenotype is caused by a second mutation in *pdr5*$_{S558Y}$	33
Figure 2	Experimental strategy designed to determine whether a suppressor is due to a second-site mutation in *pdr5*$_{S558Y}$.	41
Figure 3	Location of suppressor mutations in Pdr5. Mutations that suppress S558Y (TMH2) are shown on a 2-D topological diagram of Pdr5	45
Figure 4	An alignment of 20 members of the Pdr5 subfamily of fungal ABC transporters	46
Figure 5	The Q-loop region motif	46
Figure 6	Quantitative analysis of drug resistance in suppressor mutants	49
Figure 7	Phenotypic features of the E244G and Q951G mutations	51
Figure 8	The ATPase activity of single and double mutants	56
Figure 9	The GTPase activity of WT, E244G, and E244G, Q951G	58
Figure 10	Characterization of E1013A and G312A	62
Figure 11	Pdr5 mediated ATPase activity in WT and mutant strains	64
Figure 12	Intergenic suppressors of E1013A clotrimazole hypersensitivity -Spot test	67
Figure 13	Intergenic suppressors of E1013A clotrimazole hypersensitivity - Quantitative analysis	68
Figure 14	Intergenic suppressors of E1013A clotrimazole hypersensitivity -Immunoblot	69
Figure 15	ATPase activity of SUP5 and SUP6	71

LIST OF TABLES

Table 1	Location of suppressor mutations	45
Table 2	Summary of important phenotypic characteristics	57
Table 3	Microarray Data	73

ABBREVEATIONS

5-FOA	5-Fluoroorotic Acid
ABC	ATP binding cassette
ADP	adenosine diphosphate
ATP	adenosine triphosphate
BCA	bicinchoninic Acid
CDR	Candida drug resistance
CFTR	cystic fibrosis transmembrane conductance regulator
Clo	clotimazole
Cyh	cycloheximide
DNA	deoxyribonucleic acid
DTT	dichlorodiphenyltrichloroethane
EDTA	ethylenediaminetetraacetic acid
EGTA	ethylene glycol tetraacetic acid

ER	endoplasmic reticulum
FACS	fluorescence-activated cell sorting
G-418	geneticin
IAAP	iodoarylazidoprazosin
LB	Luria-Bertani media
MDR	multi drug resistance
MIC	minimum inhibitory concentration
MOPS	3-(N-morpholino) propanesulfonic acid
MRP	multi drug resistance- associated protein
NBD	nucleotide binding domain
ORF	open reading frame
PAGE	polyacrylamide gel electrophoresis
PBS	phosphate buffered saline
PBST	phosphate buffered saline with tween 20
PDR	pleotropic drug resistance

Pgp	P-glycoprotein
Pi	inorganic phosphate
PMSF	phenylmethyl sulfonyl fluoride
R6G	rhodamine 6G
RPM	revolutions per minute
SD	synthetic dextrose
SDS	sodium dodecylsulfate
TAP	transporter associated with antigen processing
TMD	transmembrabe domain
TPCK	L-1-Tosylamide-2-phenylethyl chloromethyl ketone
URA	uracil
UV	ultraviolet
YPD	yeast peptone dextrose

INTRODUCTION

Structure of ABC transporters

ATP Binding Cassette (ABC) proteins constitute one of the largest membrane transporter superfamily. ABC proteins are present in every living cell ranging from bacteria to higher eukaryotes (Dean *et al.,* 2001). These transporters use ATP as a source of energy to translocate a broad range of substrates across the plasma membrane. They can function as importers (example: vitamin B_{12} importer, BtuCD), transporting nutrients and ions into the cell or as exporters (example: mammalian multi drug efflux pump, P- glycoprotein) which pump toxins and drugs out of the cell. ABC transporters have gained importance as they often contribute to multidrug resistance in microbial pathogens and tumor cells impeding treatment of infectious diseases and cancer. (Peddlock *et al.,* 2006). There are 48 ABC transporters in humans and mutations in many are the root of genetic disorders like cystic fibrosis (lung and gut), Tangier disease (cardiovascular) and Dubin-Johnson syndrome (liver).

ABC transporters are composed of four core domains; two transmembrane domains (TMDs) and two nucleotide binding domains (NBDs). The transmembrane domains are embedded in the membrane bilayer and contain substrate binding sites. The nucleotide binding domains are located in the cytosol. They bind/hydrolyze ATP that provides energy for substrate transport. While most ABC proteins exist as full transporters with two NBDs and two TMDs, some ABC proteins occur as half

transporters that are made up of only one TMD and one NBD. These half transporters are thought to homo- or hetero- dimarize to form a functional full transporter (Dean *et al.*, 2001).

Transmembrane Domains: A 'typical' ABC transporter contains 12 transmambrane helices. They are membrane spanning α-helices which come together to form a channel through which substrates are transported (Higgins *et al.*, 2001 and Rea *et al.*, 1999). The TMDs possess substrate binding sites. Some ABC transporters may have additional domains that regulate the protein function by conferring additional specificity or imparting transport directionality (Higgins *et al.*, 2001). The sequences and architecture of the TMDs are variable, reflecting mechanistic differences in function and chemical diversity of the translocated substrates. ButD and MsbA are the only two ABC transporters for which high resolution TMD structures are available (Roth et al., 2001). The TMDs of the two proteins show little sequence homology and cannot be modeled on each other. Furthermore the transmembrane helices are connected to each other by intracellular loops (ICLs) and extracellular loops (ECLs).

Nucleotide Binding Domains: A functional transport protein contains two NBDs. Both the NBDs come together to form two ATP binding sites. The NBDs contain conserved sequences that position ATP, catalyze its hydrolysis, and communicate this signal to drug-binding sites in the TMDs. These include, among

others, the Walker A motif (GXXGXGK(S/T)), Walker B motif (ΦΦΦΦD, where Φ is a hydrophobic residue), Q-loop, and signature motif (LSGGQ). Crystal structures solved for the complete transporter Sav1866 supports a model in which the NBDs come together in a head-to-tail orientation such that an ATP molecule is sandwiched between the Walker A, B, and Q-loop sequences of one NBD and the signature and of the other (Seeger *et al.,* 2009). The NBD orientation and ATP binding sites were also crystallographically characterized for the non transporting ABC transporter Rad50 (Hopfner *et al.,* 2000). In this complex, the nucleotide is occluded in a nonexchangeable manner, and subsequent hydrolysis appears to be necessary for the disassembly of the sandwich (Sauna *et al.,* 2006). It is generally observed that in the ATP bound state the NBDs are closely associated with each other, where as a nucleotide free transporter exhibits a conformation with greater separation between the NBD.

Energetics of transport

Extensive studies of ATP catalytic cycle linked to drug affinity data make P-gp the best characterized ABC transporter. These biochemical data along with structural studies are the bases for the ATP-sandwich model to explain the kinetics of ATP binding/hydrolysis and substrate transport in ABC transporters.

Step I: Ligand binding to the TMDs

Substrate binding studies done with P-glycoprotein and LmrA (Sauna *et al.,* 2000 and VanVeer *et al.,* 2000) suggest that transporters have high affinity for ligands in a nucleotide free environment. Binding of the ligand at the TMD is thought to cause a conformational change in the NBD (Kreimer *et al.,* 2000 and Liu *et al.,* 1996). Upon ligand binding a signal is transduced from the TMDs to the Q loop of the NBD through the ICLs. Crystal structure of HlyB and LolD suggest that Walker A is displaced in response to the signal transmitted from the TMDs that allows ATP to gain access to the nucleotide binding site. The signature motif from the other NBD aligns with the rest of the nucleotide binding pocket and a closed dimer is formed.

Step II: Closed dimer formation – power stroke for transport

Structural and biochemical studies suggest that ATP binding at the NBD induces the formation of closed dimer, which in turn results in a substantial conformational change in the TMDs leading to substrate release. Structural data from P-gp and MutS show two molecules of ATP at the NBD dimer interface, implying that they act in concert (Smith *et al.,* 2002). NBD dimer formation induced by ATP binding generates a significant amount of free energy (Smith *et al.,* 2002). This energy is translocated to the TMDs resulting in its reorientation. This

conformational change has been visualized in P-gp (Rosenberg *et al.,* 2001). Binding of a non-hydrolysable ATP analog to P-gp was sufficient to cause rearrangement of the TMDs thereby altering the affinity of the substrate (vinblastin) at the binding site (Martin 2001). In CFTR, ATP binding was sufficient to open the chloride channel (Vergani *et al.,* 2005).

Step III: ATP hydrolysis

The transient nature of the NBD dimers formed by ATP binding suggests that hydrolysis is an imminent part of dimer formation. ATP hydrolysis destabilizes the dimer and initiates resetting of the transporter. The post- hydrolytic ADP+ P_i state, has a confirmation distinct from ATP-bound and nucleotide-free forms (Martin *et al.,* 2000 and Rosenberg *et al.,* 2001). In ABC transporters like CFTR and Mrp1, hydrolysis of only one ATP is sufficient to reset the transporter (Aeksandrov *et al.,* 2000). However in P-gp, hydrolysis of ATP is necessary to complete the transport cycle (Senior *et al.,* 1995).

Step IV: Release of P_i and ADP

Hydrolysis of ATP at the NBD leads to the formation of ADP and P_i. The closed NBD dimers are destabilized by electrostatic repulsion between ADP coordinated with Walker A of one NBD and P_i coordinated with signature of the other NBD (Smith *et al.,* 2002). This leads to release of ADP and P_i and the NBDs

return to the open dimer confirmation. In P-gp, vanadate can be trapped with ADP in the transition state conformation suggesting that P_i is released before ADP (Martin *et al.*, 2001). Notably, failure to release ADP prevents the NBDs to return to the open state conformation. In P-gp, ADP release can be a rate limiting step in the ATPase cycle (Senior *et al.*, 1995). It has been shown that ADP bound conformation differs from the ADP + P_i bound state (Martin *et al.*, 2002).

Asymmetric ABC transporters

P-gp and Sav1866 are examples of symmetric ABC transporters. P-gp is a full-length transporter whose two NBDs each contain a set of completely canonical motifs. Sav1866, whose atomic structure has been solved at high resolution (Locher *et al.*, 2006) is a half transporter that functions as a homodimer. In fact, many ABC transporters are asymmetric in which the two NBDs do not contain equivalent motifs.

Cystic fibrosis transmembrane conductance regulator (CFTR)

Cystic fibrosis transmembrane conductance regulator (CFTR) is an ion channel that transports chloride ions across the membrane. CFTR is encoded by a gene that belongs to subfamily-C in the ABC superfamily of proteins (Riordan et. al 1989). Mutations of the CFTR gene affect functioning of the chloride ion channel leading to cystic fibrosis. Like all ABC transporters, a full length CFTR protein incorporates

two nucleotide binding domains (NBDs). Interestingly, like Pdr5, NBD1 is made up of deviant sequences and NBD2 is canonical. In CFTR, the catalysis of ATP at the NBD is thought to power conformational change at the TMD essential for transport function. However, the mechanistic details of the link between ATP hydrolysis and protein function is unknown. Basso *et al.,* (2003) used photoactivable nucleotides to gain insight into the functional mechanisms of the CFTR ATPase activity.

Studies done with other ABC-C family members that have one deviant NBD, suggest that only the canonical NBD (NBD2), but not the deviant NBD (NBD1), can hydrolyze ATP (Chang *et al.,* 1998). Gao *et al.,* (2000) showed that ATP hydrolysis in MRP1 occurs primarily at the canonical NBD (NBD2). Similarly, in SUR1, although both NBD's could be photolabeled with [α ^{32}P] ATP, only NBD1 (deviant NBD) was photolabeled by [γ ^{32}P] ATP, suggesting that hydrolysis occurs at the canonical NBD, but not at the deviant NBD (Ueda *et al.,* 1997). Photolabeling studies in CFTR by Aleksandrov *et al.,* (2002), demonstrate a similar pattern of labeling, where only the deviant NBD could be labeled with [α ^{32}P] ATP, implying hydrolysis occurs at the canonical NBD. Basso *et al.,* (2003) found that ATP can bind to the deviant NBD in a non-hydrolysable fashion; more interestingly, the nucleotide can remain occluded at NBD1 through many CFTR gating cycles. The apparent failure of NBD1 to hydrolyze ATP could be due to the presence of deviant residues in the conserved catalytic motifs. These include a serine (S573) in the deviant NBD instead of a conserved glutamate as in the canonical Walker B. (Hung *et al.,* 1998). Basso *et al.,* (2003) suggest that association and dissociation of nucleotide at the deviant NBD together with ATP hydrolysis at the canonical NBD underlines the mechanism by

which the CFTR channel functions. Also, phosphorylation of CFTR by PKA is thought to have little effect on binding/retention/hydrolysis of ATP at NBD's but is required to fine tune protein function (Basso *et al.,* 2003).

Transporter associated with antigen processing (TAP)

Transporter associated with antigen processing (TAP) is a member of the ATP-binding-cassette transporter family. It delivers cytosolic peptides into the endoplasmic reticulum (ER), and is required for the assembly of MHC class I molecules (Knittler *et al.,* 2001).The TAP functional complex is a hetrodimer formed of two proteins: TAP-1 and TAP-2, which have one transmembrane domain and one nucleotide binding domain each (Antoniou *et al.,* 2003). The two NBDs in Tap 1/2 form two ATP binding sites. Similar to Pdr5 and CFTR, TAP1/2 contains one deviant and one canonical ATP binding site (Perria *et al.,* 2006). The deviant Walker B in TAP1 contains Asp 668 in place of a highly conserved glutamic acid and Gln 701 in the deviant switch region instead of a conserved histadine. The significance of these deviant residues still remains a question. Perria *et al.,* (2006) demonstrated that a double deviant Walker B switch region mutant (D668E, Q701H) showed slightly improved ATPase activity. This indicates that the presence of Asp668 and Gln 701 contributes to natural attenuation of ATPase activity at the TAP1 site. [α ^{32}P] ATP and [γ ^{32}P] ATP nucleotide trapping suggested that ATP hydrolysis occurs at both sites in the TAP1/2 complex (Chen *et al.,* 2003). However, the trapping studies could reflect the steady state ATPase activity rather then ATP hydrolysis at each site.

Perria *et al.,* (2006) described a mechanism that suggests that the energy required for peptide translocation by the TAP1/2 complex is provided by the TAP2 canonical NBD. The deviant motifs in TAP1 show reduced catalysis indicating that ATPase activity at the TAP2 site is sufficient for protein function (Ernst *et al.,* 2006). Interestingly, chimeric TAP complexes, containing two canonical TAP2 NBDs were significantly less active than chimeric TAP complexes containing two deviant TAP1 NBDs (Arora *et al.,* 2001). Lapinski *et al.,* (2001) showed that the presence of TAP1 deviant NBD is critical for nucleotide binding at the of TAP2 canonical NBD. The data suggest that both TAP1 deviant NBD and TAP2 canonical NBD are required for efficient catalytic cycle and peptide translocation; TAP2 contains all the catalytic active residues critical for ATP hydrolysis, however, TAP1 NBD is essential for optimal nucleotide binding and initiation of the catalytic cycle at the TAP2 site.

LmrCD

LmrCD is a multidrug ABC transporter from *Lactococcus lactis.* It is a heterodimeric transporter made up of two half transporters, LmrC and LmrD. LmrCD is an asymmetric transporter containing one canonical ATP binding site and one deviant ATP binding site. The canonical Walker B of LmrD has a catalytic glutamate (Glu587), but, in LmrC it is substituted for an aspertate (Asp495). Lubelski *et al.,* (2005) demonstrated that the heterodimeric NBDs of LmrCD are structurally and functionally different. Glu 587 of LmrD is thought to be important for catalysis, while the function of Asp 495 in LmrC is unknown. $LmrC^{D495Q}$/ LmrD mutation retained

considerable ATPase activity, whereas, LmrC/LmrD^{E587Q} completely abolished protein function Lubelski *et al.*,(2005). Drug efflux studies also indicated that mutation in LmrD caused severe drug sensitivity. 8-azido-[α-^{32}P]ATP cross linking experiments showed asymmetric labeling, with heavy labeling of LmrC (Lubelski *et al.*,2005). Asymmetric labeling has also been demonstrated for non equivalent NBDs of MRP1 (Chen *et al.,* 2003), CFTR (Basso *et al.,* 2003) and TAP (Carrier *et al.,* 2003), indicating a similar mechanism of function. The asymmetry of the motifs in the NBDs of LmrC and LmrD suggest a functional non equivalency with both the NBDs performing different roles. It appears that two ATP molecules can bind to LmrCD, however only one is rapidly hydrolyzed while the other may play a role in regulation (Lubelski *et al.,* 2005).

Phylognetic classification of ABC transporters

ABC-A (Subfamily A)

A characteristic feature of ABC-A is the presence of a regulatory domain after the NBD. The regulatory domain has phosphorylation sites required for protein activation. This subfamily is also characterized by the presence of a large extracellular loop between the first and second TMHs of both NBDs.

The ABC-A subfamily consists of both full length transporters (group I) and half transporters (group II). This subfamily is best characterized in vertebrates. The vertebrate ABC-A contains some of the largest ABC genes, with several comprised

of 2,100 amino acids. Mammalian ABCA1 protein that play a crucial role in cholesterol transport and lipid biosynthesis has been extensively studied (Wenzel *et al.*, 2007). Fungal ABCA1, though not well characterized, similar to its mammalian counterpart is required for lipid transport. There is an uneven distribution of this subfamily in the fungal genome, suggesting that these transporters are not essential for cell viability.

ABC-B (Subfamily B)

ABC-B represents a widely studied group of ABC transporters that include both full and half transporters. They are characterized by the presence of a central NBD and an N-terminal NBD. They are abundantly distributed among eukaryotes and have diverse functions. ABCB1 (P-gp) is a widely studied member of this group. ABCB1 functions at the blood brain barrier in the liver and has the ability to confer resistance to cancerous cells. Two half transporters, ABCB2 and ABCB3, form heterodimers responsible for transporting peptides that will eventually be presented as antigens by the Class I HLA molecules. ABCB6, ABCB7, ABCB8 and ABCB10 are all half transporters that localize to the mitochondria and take part in iron metabolism (Frank *et al.*, 2003).

ABC-C (Subfamily C)

Subfamily C members are full length transporters found in eukaryotes. These proteins are characterized by the presence of an additional N terminal hydrophobic extension. Some ABC-C transporters function as ATP gated ion channels. Most notable among them is the cystic fibrosis transmembrane conductance regulator (CFTR) protein that in humans is encoded by the *CFTR* gene. The CFTR gene encodes an ion channel that transports chloride ions across the cell membrane. Mutations of the CFTR gene affect functioning of the chloride ion channels, leading to cystic fibrosis. In humans many members of this subfamily (ABCC1, ABCC2, ABCC3, ABCC4, ABCC5 and ABCC11and ABCC12) are transportes implicated in drug resistance. ABCC8 and ABCC9 proteins function to modulate insulin secretion and maintain normal levels of insulin the body (Annilo *et al.,* 2005).

ABC-D (Subfamily D)

ABC-D members subfamily encode half transporters that homo- and/or hetero- dimerize to form functional transporters that localize to the peroxisomal membrane. They mediate the import of long-chain fatty acids. *S. cerevisiae* has two transporters that belong to this family, Pxa1p and Pxa2p (Driessen *et al.,* 2010). They function as heterodimers and play an important role in palmitate metabolism in the cell.

ABC-E and ABC-F (Subfamily E and F)

Subfamily E and F members are soluble ABC proteins. They solely contain two NBDs and lack TMDs. There function within the cell is not related to transport. However they are included in the ABC superfamily due to their homologies with the NBDs. Ril1, Arb1, Yef3 are members of this subfamily and are essential for the survival of *S. cerevisiae.* ABC-E proteins have been identified in genomes of fungi and other eukaryotes. Ril1 well studied protein in *S. cerevisiae* is an iron-sulfur protein that is required for ribosome biogenesis (Rotte *et al.,* 2005). ABC-F proteins are required for ribosome biogenesis, mRNA export, translational control or act as translational elongation factors (Driessen *et al.,* 2010).

ABC-G (Subfamily G)

The characteristic feature that distinguishes ABC-G transporters from other subfamilies is their reverse topology. This subfamily includes both full and half transporters. ABC-G proteins are extensively studied as several of these transporters are linked to pleiotropic drug resistance (PDR) phenomena (Cannon *et al.*, 2009). Hence the full-length proteins are often referred to as PDR transporters. The half-length transporters are often called WBC transporters after the white brown complex transporters from *D. melanogaster* that are required for eye pigmentation (Driessen *et al.,* 2010). There are ten full-length PDR transporters in *S. cerevisiae* out of which Pdr5 and Snq2 are extensively studied (Goffeau *et al.,* 1995). The

function of three transporters (Adp1, Pdr18 and YOL075C remain unknown (Driessen *et al.,* 2010).

ABC transporters in yeast

Whole genome sequencing of non-pathogenic, bakers' yeast *Saccharomyces cerevisiae* and pathogenic *Candida albicans* has led to the identification and classification of many protein transporters that belong to the ABC superfamily. These transporters serve as the first line of defense and help in yeast detoxification by effluxing out xenobiotics from the cell. Amongst the many ABC transporters in yeast, PDR (Pleotropic Drug Resistance) and MDR (Multi Drug Resistance) subfamilies have been well characterized (Goffeau *et al.,* 1997). These proteins are localized in the membrane of important organelles like the plasma membrane, Golgi, mitochondria, endoplasmic reticulum etc. The presence of a large number of ABC efflux pumps in the yeast genome suggests a fundamental physiological role of these proteins. ABC proteins in yeast perform a host of functions like drug transport, ion homeostasis, heavy metal detoxification, sterol homeostasis etc (Prasad *et al.,* 2002).

ABC transporters in *Saccharomyces cerevisiae*

There are 31 putative ABC transporters in *Saccharomyces cerevisiae* with different topology and composition. The number of amino acid residues in the ABC

transporters of *Saccharomyces cerevisiae* range between 289 and 1661 residues (Decollignies *et al.,* 1997). These ABC proteins can be full transporters or half transporters with either forward or reverse topology. On the basis of phylogenetic analysis, *Saccharomyces* ABC transporters can be classified into three distinct subfamilies, MDR (Multi Drug Resistance), MRP (Multi Drug Resistance-associated Protein) and PDR (Pleotropic Drug Resistance) (Goffeau *et al.,* 1997).

The MDR and MPR subfamilies have the forward topology (TMD-NBD) while the PDR subfamily has the reverse topological orientation (NBD-TMD). Among the MDR subfamily Ste6p (Sterile 6) that transports pheromones, is the only full length transporter $(TMD\text{-}NBD)_2$ (McGranth *et al.,* 1989). Atm1p (ABC transporters of mitochondria 1), Mdl1p (Multidrug resistance like protein 1), Mdl2p (Multidrug resistance like protein 1) are all half transporters that localize to the inner membrane of the mitochondria (Dean *et al.,* 1994).

Molecular modeling of Pdr5

The Pdr5 family of fungal transporters possess a number of unique features that include a deviant ATP binding site, reverse topology, long interconnecting intracellular and extracellular loops, and low sequence identity among the transmembrane helices. Pdr5 also displays sequence and functional homology to clinically relevant ABC proteins such as Cdr1 from *Candida albicans* and Cgr1 from *Candida glabrata* thus making Pdr5 an important model transporter to study drug

resistance. The unique features along with its clinical relevance make Pdr5 an interesting protein to model.

Since X-ray crystal structures of membrane proteins are very difficult to obtain, Rutledge *et al.,* (2011) developed a molecular model of Pdr5 that provides important spatial information and insightful data into mechanisms of Pdr5 function. This computational model of Pdr5 provided necessary information to understand the communication between the transmembrane helices and the nucleotide binding domains and also interaction between Pdr5 and substrate/nucleotide (Rutledge *et al.,* 2011).

Modeling of transmembrane helices (TMH's)

Rutledge *et al.,* (2011) used the crystal structure of Sav1866 (Locher *et al.,* 2007) and P-glycoprotein (Aller *et al.,* 2009) as a template to model the TMH's of Pdr5. Their data showed that TMH's of Pdr5 align well with Sav1866. However, the last two TMH's fail to align as Sav1866 has longer interconnecting loops than Pdr5. Aller *et al.,* (2009) showed that a similar mismatch occurred when P-gp was used as a template to model Pdr5. The TMH's of Pdr5 share 36% sequence similarity with P-gp and 28.9% sequence similarity with Sav1866. The low sequence similarity is because Sav1866 is a bacterial half transporter and P-gp is a mammalian transporter with forward topology; whereas Pdr5 is a yeast multidrug transporter with a reverse topology (Rutledge *et al.,* 2011).

As the templates used had low sequence similarity Rutledge *et al.,* (2011) validated their modeling data with biochemical evidence. The Pdr5 model suggests that the 12 TMHs come together to forma a channel that traverse the membrane, enclosing a large central cavity. Residues from TMH's 1,3,6,7 and 9 form the central cavity and contribute to the formation of substrate binding pockets. The Pdr5 model by Rutledge *et al.,* (2011) predicted that Thr1213 and Gln 1253 from TMH 7 and 8 respectively form the part of the drug binding pocket. These residues are thought to bind a number of drugs because of their ability to form hydrogen bonds (Hanson *et al.,* 2005). Mutating Thr1213 and Gln 1253 to alanine resulted in severe cyh and clo sensitivity thus providing support for the model that Thr1213 and Gln 1253 are the part of substrate binding pocket (Rutledge *et al.,* 2011). Sauna *et al.,* (2008) showed that a Ser to Tyr mutation at residue 558 in TMH-2 causes loss of communication between the TMD's and NBD's. Consistently, the Pdr5 model by Rutledge *et al.,* (2008) also showed that Ser558 does not contribute to the drug binding pocket and may be important in signaling.

Modeling of the nucleotide binding domains (NBD's)

NBD of hemolysin B of *E.coli* is thought to be the closest homology of Pdr5 NBDs with 19.4% identity and 45% similarity to NBD1 and 23.7% identity and 50.9% similarity to NBD2 (Rutledge *et al.,* 2011). The well known mammalian ABC transporter P-gp shares 19.4% identity and 41.3% similarity with NBD1, and 20.2% identity and 45.7% similarity with NBD2 (Rutledge *et al.,* 2011).

The NBDs of Pdr5 come together to form two ATP binding sites, each site being a composite of both NBDs. The ATP binding sites are lined by highly conserved sequence motifs that help bind, position and hydrolyze ATP. One ATP binding site is normal and made up of canonical residues; however the second ATP binding site is made up of deviant motifs. Apart from Pdr5, other well characterized proteins like Mrp1 (Qin *et al.,* 2008) and Cdr1 (Jha *et al.,* 2004) also contain deviant NBD motifs.

The canonical Walker A motif in NBD2 is occupied by the classical Lys residue (Gly-X_4-Gly-Lys-[Ser/Thr]). The NBD1 walker A however has a cysteine in place of the typical lysine residue. The change from Cys to Lys is dramatic due to the different properties of Cys and Lys and this change could affect the structure and function of NBD1 (Rutledge *et al.,* 2011). The positively charged Lys has the ability to form a hydrogen bond with the β and γ- phosphate of ATP, facilitating the hydrolysis of nucleotide (Rutledge *et al.,* 2011). Cysteine, on the other hand, is a short negatively charged residue and is incapable in catalyzing hydrolysis. Interestingly the cysteine in the deviant Walker A is well conserved in the Pdr5 family of fungal transporters.

The deviant Walker A from NBD1 along with the equally deviant signature motif from NBD2 forms an ATP binding site. The signature motif is speculated to interact with the γ-phosphate of ATP. The NBD1 has a canonical signature sequence (Val-Ser-Lys-Glu-Glu). In contrast, the sequence of the deviant signature is completely different (Leu-Asn-Val-Glu-Gln). Interestingly, the residues that make up

the deviant signature in NBD2 are much larger than the canonical signature in NBD1 (Rutledge *et al.,* 2011). The most dramatic difference in terms of size and charge is Gly-312 in NBD1 and its equivalent residue Glu-1013 in NBD2. The negatively charged acidic residue is speculated to repel the γ-phosphate of ATP; however this repulsion may be neutralized by the neighboring positively charged residues (Rutledge *et al.,* 2011).

The Walker B of the canonical NBD2 contains a canonical glutamate residue. This residue is known to activate a water molecule which in turn cleaves the γ-phosphate from ATP. The NBD1 of Walker B possesses an asparagine (Asn 334) instead of the usual glutamate as in NBD2.

The Q-loop in Pdr5 is thought to form a communication bridge between the TMD's and the NBD's (Ananthaswamy *et al.,* 2010). The Q-loop in NBD2 has a canonical Glutamine at position 951. This is replaced by a Glutamate (Glu244) in the deviant Q-loop in NBD1. Sauna *et al.,* (2008) identified that the deviant Q-loop residue Glu 244 along with Asn 242 and Asp 246 in the Q-loop region interact with ICL1 which connects TMH 2 and TMH 3. The crystal structure of Sav1866 (Locher *et al.,* 2007) and the computational model of Pdr5 (Rutledge *et al.,* 2011) also predict this communication interface between the Q-loop and the interconnecting loops.

Rutledge *et al.,* (2011) verified the NBD model by mutating key residues in the deviant and canonical NBD's. These mutations included Asn 242 Lys, Thr 257Ile, Gly302Asp, Gly1009Cys and His1968Ala. These mutations either affect the catalytic ATP cycle or affect the crosstalk between the NBD's and the TMD's. Taken together,

the deviant Walker A, Walker B and Q-loop from NBD1 and the deviant signature from NBD2 forms a unique ATP binding site that is evolutionary conserved in the Pdr5 subfamily. Computational modeling indicates that the deviant motifs surround an ATP molecule (Rutledge *et al.,* 2011). Complex and novel interaction between the residues of the deviant ATP binding site may be required to actively bind and hydrolyze ATP.

Defining a Signal Interface in ABC Transporters

ABC transporters are polytopic proteins with multiple domains. ATP hydrolysis occurs in hybrids of the two NBDs which are often found in the cytosol. Transport substrate binding and transport often occur in the transmembrane domains. An extremely important question is how chemical energy produced from ATP hydrolysis is channeled into mechanical force to provide the conformational changes necessary for drug transport in another location.

The crystal structure of the bacterial ABC transporter Sav1866 from *Staphylococcus aureus*, suggests a domain arrangement in which the NBDs are in contact with the TMDs (Locher *et al.,* 2006). Such an interaction indicates coupling and communication between the two domains in which energy generated from ATP binding/hydrolysis is transmitted to the TMDs triggering conformational change. The mechanism by which the signal energy is transduced across the TMD: NBD interface

remains obscure. The structural data of Sav1866 predicted that the Q-loop and the x-loop (located just prior to the signature region) in NBD2 are in contact with the ICL2 of TMD1, suggesting a trans interface. ICL1 was shown to be in contact with both NBDs. (Locher *et al.,* 2006).

Sav1866 is a homolog of P-glycoprotein, a clinically relevant ABC transporter implicated in cancer. Both proteins are members of the MDR family of ABC transporters, sharing similar topology and functional domains. Due to the high homology between the two transporters it can be predicted that P-gp might have a transmission interface similar to Sav1866 (Zolnerciks *et al.,* 2007) with the long ICLs in TMD2 contacting NBD1. To biochemically test the Sav1866 structural data, Zolnerciks *et al.,* (2007) used P-gp as a template to analyze the communication between the TMDs and NBDs using cross-linking studies. Cysteine mutations generated in the Q-loop region of NBD1 (L443C and C474C) and ICL4 of the opposite NBD (S909C and R905C) suggest that the Q-loop and ICL4 are in close physical proximity in the tertiary structure of P-gp.

The transmission interface of Tap1/2 was recently investigated. A 3D structural model of the TAP complex was constructed based on Sav1866 (Tampe *et al.,* 2009) to examine the signal interface between the TMD and NBD. Based on this, the investigators made a cysteine substitution for a conserved glutamate in the X-loop and the carried out cysteine scan mutagenesis on residues in ICL1 and ICL2. Cross-linking studies with these some of combinations rendered Tap1/2 transport complex

incompetent thus demonstrating that the X-loop in the TAP NBD interacts with ICL1 and 2 in the TMD of the opposite half transporter.

Preliminary work (Sauna *et al.* 2008) demonstrated an interaction between a residue in TMH2 and one very near the Q-loop of Pdr5 (N242K) suggesting that even this deviant transporter has an interface similar to other ABC proteins. A major goal of the research described below is to identify additional residues that participate in this critical function through suppressor analysis and examine the effect of altering these through site-directed mutagenesis.

MATERIALS AND METHODS

A. Strains, Plasmid, Media and Drugs

All yeast strains used in the study are derivatives of the R-1 strain. In R-1 the PDR5 coding region was removed and replaced by a geneticin cassette. A copy of PDR5 with a desired mutation was introduced of R-1 via mutagenesis and transformation with an integrating plasmid (pSS607). This plasmid has a wild type copy of Pdr5 including all of the regulatory sequences required for expression in yeast. The URA3 gene serves as a selectable marker for transformation into R-1 which is ura3 and otherwise requires uracil in its growth medium.

The yeast and bacterial cells were either grown in complete medium with/without selection component or in synthetic dropout media. The reagents for the media were obtained from MidSci (St.Louis, MO). The media was prepared by dissolving the required regents in reverse osmosis water (RO-H_2O) and sterilized by autoclaving at 121 °C and 15 psi for 20 min.

YPD (yeast extract, peptone, dextrose) broth medium was composed of 20 g dextrose, 20 g peptone and 10 g yeast extract per liter of water. Solid YPD agar was made by adding 20 g of agar to 1liter of YPD broth. SD (synthetic defined) broth contained 20 g dextrose, 7 g yeast nitrogen base without amino acids and 0.1 g of the required amino acid per 1 liter of water. For solid media 20 g agar was added per liter of SD broth. LB (Lauria-Bertani) broth media was prepared by adding 10 g tryptone, 5 g

yeast extract and 10 g sodium chloride in 1 liter of water. 20 g per one liter agar was added to prepare solid medium.

Drug/selective medium was prepared by adding the required chemical to the various media listed above. After sterilization the medium was cooled to 55 °C before addition of the appropriate drug. Geneticin (RPI Corp., Mt. Prospect, IL) was added to the YPD medium at a concentration of 200 mg/liter. Cychloheximide (Cyh) (Sigma, St. Louis,MO) was dissolved in water to prepare a stock solution of 10 mg/ml and was added to YPD media at a concentration of 0.25 to 21.6 µM. Clotrimazole (Clo) (Sigma, St. Louis,MO) was dissolved in DMSO to prepare a stock solution of 10 mg/ml which was added to YPD at a concentration of 1.25 to 25.0 µM. 5FOA (5-fluorooratic acid) medium was prepared by adding 250 mg 5-fluorooratic acid (RPI Corp., Mt. Prospect, IL) to SD medium. Ampicillin (Amp) (Fisher Scientific, Fair Lawn, NJ) was dissolved in water to prepare a concentration of 50 mg/ml and 50 ug/ml was added to LB agar. All yeast strains were grown at 30 °C and *E.coli* was grown at 37 °C.

B. Primers

Primers for site directed mutagenesis were designed using the website www.primerx.com, and synthesized by Operon (Huntsville, AL).

C. Sequencing of PDR5 gene

Saccharomyces Genome Database (www.yeastgenome.org) was used to design overlapping primers to sequence the entire PDR5 ORF. The DNA samples to be sequenced were sent to Retrogen Inc. (San Diego, CA) for sequencing. The sequence

obtained was translated using Swiss Protein Database website (www.expasy.org/translate/) and compared to the PDR5 sequence from the *Saccharomyces* Genome Database using the blast function to confirm the location of the desired mutation.

D. Electrophoresis

Agarose gel electrophoresis

1% agarose gels were prepared by mixing 1 g of agarose in 100 ml of 1X Tris-acetate buffer (for 50X stock: 242 g tris base,57.1 ml acetic acid and 100 ml 0.5M EDTA was mixed and made up to 1 L with distilled water). The agarose was dissolved by boiling in a microwave. 10 µl of 10 mg/ml ethidium bromide was added. The agarose was poured into gel molds and combes were placed in appropriate locations to form wells. Once set, the gel was placed in electrophoresis chamber containing 1X Tris-acetate buffer.

Sample was prepared by mixing 5 ul of DNA and 1 µl of loading dye (Ambresco, Solon, OH). The total volume was made up to 10 µl using distilled water. The sample and Lambda *HinD* III ladder (Promege, Madison,WI) were loaded into the wells of the agarose and run at 100 V for 1 hr, until the loading dye progresses to the edge of the gel. Following electrophoresis the gel was visualized under UV light to observe the DNA bands.

Protein gel electophoresis

SDS-PAGE gels are run to confirm the presence of Pdr5p in the purified plasma membranes. The amount of plasma membrane sample required to obtain 30 µg of protein was calculated. A volume of SDS equivalent to $1/4^{th}$ the volume of plasma membrane protein was added. The sample was incubated at 42 ºC for 25 min.

The sample was loaded onto a 7% Tris acetate gel (Invitrogen, Carlsbad, CA) and run at 150 V until the dye ran off the gel. The gel was then removed from the cassette and transferred to a staining tray. The gel was first fixed with 10% acetic acid for 10 min and then stained using the Colloiadal Blue Stain Kit (Invitrogen, Carlsbad, CA) for 1 hr. The gel was distained overnight in reverse osmosis water. The following day, the gel was observed for the presence of the protein band representing Pdr5 (160kDa).

E. Polymerase Chain Reaction

Site Directed Mutagenesis of PDR5 in pSS607

Quick Change XL site directed mutagenesis kit (Stratagene, La Jolla, CA) was used to make point mutations and amplify the mutated vector DNA. PCR (polymerase chain reaction) samples were prepared as follows:

10X Reaction buffer	5 µl
Forward primer	125 ng
Reverse primer	125 ng
dNTP	1 µl
Quick solution	3 µl
Pfu Turbo polymerase	1 µl
Template plasmid-pSS607	10 ng

The total volume was made up to 50 µl with sterile water. The sample was placed in a thermocycler (Techne-TE3000, Burlington, NJ) and cycled according to the parameters displayed below.

Segment	Cycles	Temperature	Time
1	1	95 °C	60 seconds
2	18	95 °C	50 seconds
		55 °C	50 seconds
		68 °C	14 minutes
3	1	68 °C	7 minutes
4	∞	4 °C	∞

1 µl of Dpn-I restriction enzyme (100U/ µl) (Agilent-Stratagene Technology, Santa Clara, CA) was added to the PCR amplified product. The reaction mixture was incubated for 1hr at 37 ºC to digest parental (unmutated) plasmid DNA.

Amplification of PDR5 from yeast chromosomal DNA

Qiagen Long Range PCR Kit (Qiagen,Valencia, CA) was used to make point mutations and amplify the mutated vector DNA. PCR (polymerase chain reaction) samples were prepared as follows:

Reaction buffer	5 µl
Forward primer	4 µl of 5 µM stock
Reverse primer	4 µl of 5 µM stock
dNTP	2.5 µl
Pfu Turbo polymerase	0.5 µl
Template chromosomal DNA	100 ng

The total volume was made up to 50µl with sterile water. The sample was placed in a thermocycler (Techne-TE3000, Burlington, NJ) and cycled according to the parameters displayed below.

Segment	Cycles	Temperature	Time
1	1	93 °C	3 minutes
2	40	93 °C	30 seconds
		55 °C	30 seconds
		68 °C	6 minutes
3	∞	4 °C	∞

F. Preparation of DNA

Purification of plasmid DNA from *E.coli*

Plasmid DNA was amplified in *E.coli* and recovered using the High-Speed Plasmid Mini Kit from IBI Scientific (Peosta, IA). 10 ml of LB-amp broth was inoculated with bacteria containing the plasmid of interest. The culture was grown overnight at 37 ºC with shaking. The bacteria were harvested by centrifugation in a clinical centrifuge at 6000 RPM for 5 min. The supernatant was discarded. 200 µl of PD1 (resuspension buffer containing RNAse) was added to the pellet and resuspended by vortexing. The cell suspension was then transferred to a microcentrifuge tube. 200 µl of PD2 (cell lysis solution) was added and mixed by inverting the tube 10 times and incubating the tube at room temperature for 2 min. Following this 300 µl of PD3 (neutralization solution) was added and mixed immediately by inverting the tube 10 times. The lysate was centrifuged at 14,000 RPM for 3 min. The supernatant was applied on a column placed in a 2 ml collection tube and centrifuged for 30 sec at 14,000 RPM. The plasmid DNA gets trapped in the column resin and the flow through that accumulates in the collection tube was discarded. 400 µl of W1 (wash) buffer was added to the column and centrifuged at 14,000 RPM for 10 sec. The column was again washed with 600 µl of W2 (washing containing ethanol) and centrifuged at 14,000 RPM for 30 sec. The column was again centrifuged for an additional 3min to remove all residual buffer from the filter resin. The PD column was placed in a fresh eppendorf tube. 50 µl of elution buffer was added to the center of the column matrix. The column was allowed to stand at room temperature for 2 min. DNA was eluded by centrifugation at 14,000 RPM for 2 min.

Extraction of yeast genomic DNA

Yeast chromosomal DNA was purified using the Gentra Puregene Yeast Kit (Qiagen, Valencia, CA). 10 ml of YPD broth was inoculated with appropriate strain and grown overnight at 30 ºC. The cells were pelleted by centrifugation at 16,000 RPM for 30 sec in a clinical centrifuge. The supernatant was discarded and the pellet was resuspended in 300 µl of cell suspension solution. The cell suspension was transferred to a microfuge tube. 1.5 µl of lytic enzyme solution was added and the contents were mixed. The tubes were then incubated at 37 ºC for 30 min. Following this the cells were pelleted by centrifuging at 16,000 RPM for 1 min. The supernatant was discarded and 300 µl of cell lysis solution and 100 µl of protein precipitation solution was added and vortexed vigorously for 20 sec. The precipitated protein was pelleted by centrifugation at 16,000 RPM for 3 min. The supernatant was transferred to a fresh microfuge tube containing 300 µl of isopropyl alcohol to pellet the DNA. The sample was mixed by inversion and centrifuged at 16,000 RPM for 3 min. The supernatant was removed the DNA pellet was washed with 300 µl of 70 % ethanol. The tube was centrifuged for 1min at 16,000 RPM. The DNA pellet was air dried for 10 min. 50 µl of DNA hydration solution and 1.5 µl of RNase-A was added to the DNA pellet and incubated at 37 ºC for 1 hr. DNA was then dissolved for 1hr at 65 ºC. The DNA solution was then cooled at room temperature and stored at 4 ºC.

G. Transformation Techniques

Bacterial transformation

A frozen vile of XL10 Gold ultra-competent cells (Stratagene, LaJolla,CA) was thawed on ice. 45 µl of cells were added into a pre-chilled 14 ml BD Falcon polypropylene round bottom tube (Fisher Scientific, Fairlawn, NJ) for the sample reaction and positive and negative controls. 2 µl of β-mercaptoethnol (Stratagene, LaJolla, CA) was added to each tube. The tubes were swirled and then incubated on ice for 10 min. 2 µl of the sample plasmid DNA was added into the tube. 1 µl of 0.01 ng/µl pUC was added as positive control plasmid. No plasmid was added to the negative control. The transformation mixture was swirled to mix the contents and incubated on ice for 30 min. The cells were then heat shocked by placing the tubes in a 42 °C water bath for 30 sec. Following this, the tubes were immediately cooled on ice for 2 min. 500 µl of pre-warmed LB broth was added to each sample and the tubes were incubated at 37 °C for 1 hr with shaking. The cells were plated on LB Amp plates (100 µl reaction mixture/plate) and incubated at 37 °C overnight.

Transformantion of plasmid DNA into yeast

20 ml of YPD medium was inoculated with the starter culture of the desired yeast strain. The cells were grown at 30 ºC with shaking until they reached stationary phase. This culture was diluted into 100 ml YPD medium in a 500 ml flask so that the OD_{600} was 1.0. The cells were harvested by centrifugation at RT for 5 min at 5000 RPM in a Sorval centrifuge using a SS-34 rotor. The supernatant was discarded and the cell pellet

was resuspended in 50 ml of sterile water and centrifuged again. Following the wash the cells were resuspended in 1 ml of transformation buffer. The required number of sterile microfuge tubes were set up; one for each transformation and one each for positive and negative control. 10 µl (10mg/ml) of single stranded salmon testes DNA was added into each tube. pUC plasmid was used as a positive control. No plasmid was added to the negative control. 100 µl of competent cells in transformation buffer was added to each microfuge tube and vortexed. 600 µl of PLATE buffer was added to the reaction mixture. The tubes were incubated at 30 °C for 30 min with shaking. The cells were then heat shocked at 42 °C for 15 min. Following the heat shock the cells were pelleted at top speed in a micro-centrifuge for 3 sec. The supernatant was discarded and the cells were resuspended in 500 µl of sterile water. 100 µl of this suspension was plated on an appropriate medium and the plates were incubated at 30 °C for 3-4 days.

5FOA testing and selection on G-418

The experimental strategy for 5FOA testing and selection on geneticin (G-418) is described in Figure 1.

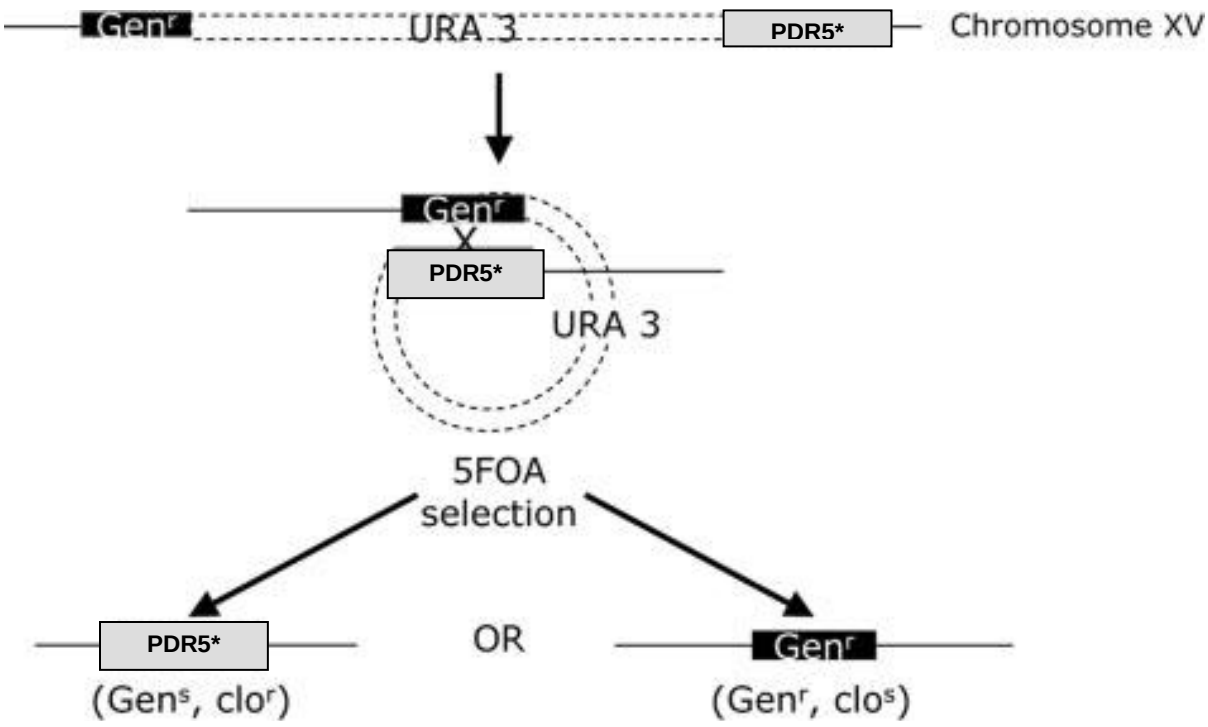

FIGURE 1. Experimental strategy to determine whether a reversion phenotype is caused by a second mutation in pdr5S558Y. In this illustration, it is assumed that the new mutation (*) lies in PDR5. Loss of the plasmid sequences containing URA3 and 1 of 2 PDR5 cassettes, either PDR5 or pdr5::KANMX4 (GEN^r), occurs by recombination in one of the two homologous regions. These events result in Ura^- colonies that are selected on 5-FOA medium and are tested on YPD and geneticin medium. Geneticin sensitive colonies indicate successful transformation as the cassette was replaced by a PDR5 coding region.

5FOA testing and selection on G-418 was performed as follows: The desired transformant was grown overnight in 5ml YPD at 30 ºC with shaking. The cells were

pelleted in a clinical centrifuge and the supernatant was discarded. The cells were washed in 5 ml of sterile water and resuspended in 1 ml sterile water. 1:100 dilution was made and 3 samples of 50 µl were spread on 5FOA plate and incubated for 72 hrs at 30 ºC. Colonies that grew on 5FOA media were picked on to YPD and G-418 media. The plates were incubated for 72 hrs at 30 ºC. G-418 sensitive colonies indicate successful transformations were selected for further study.

H. Drug Sensitivity Testing

Spot test

Spot test was performed to quantify the differences in drug sensitivities of mutant and wild type strain. The desired yeast strains are grown in 5 ml of YPD at 30 °C with shaking. The cells were pelleted in a clinical centrifuge. The cells were washed with 10 ml of sterile water and then resuspend in 1ml of sterile water. The A_{600} of 1:100 dilution was determined. This was done by taking 10 µl of sample in a cuvette and adding 990 µl of water. A dilution that would be required to have $5X10^6$ cells/5µl was calculated. A 10 fold serial dilution was made. 5 µl of each serial dilution was spotted on appropriate drug media. The plates were incubated at 30 °C for 48 hrs. As a growth control the strains were also spotted on YPD media without drugs.

IC-50 in liquid culture

10 ml YPD broth was inoculated with the desired yeast strains in a 15 ml clinical centrifuge tube. The cultures were grown overnight at 30 °C with shaking. The absorbance of the overnight culture was measured at 600 nm, to determine the number of cells in 1 ml of the broth. A volume containing $0.5X10^5$ cells was removed and added to 2 ml YPD broth containing Clo (0-25.0µM) or Cyh (0-21.6µM). The tubes were incubated at 30 °C for 48 hrs with shaking. After 48 hrs the final cell concentration in the tubes was measured by determining the absorbance at 600 nm. Cell growth in drug media was compared to growth in plain YPD. Percentage growth-untreated control vs. concentration of drug was plotted on the graph to determine the IC 50 of the strain.

Rhodamine 6G transport assay

10 ml YPD broth was inoculated with the desired yeast strains. The cells were pelleted by centrifugation at 14,000 RPM and washed with sterile water and then with 0.5 M Hepes buffer (pH 7.0). The cells are then resuspended in 10 ml of 0.5 M Hepes buffer and the cell concentration was determined by measuring absorbance at A_{600}. A volume of broth containing $1X10^6$ cells was transferred to a fresh microfuge tube. The cells are pelleted at 14,000 RPM for 1 min in microcentrifuge. The pellets were resuspended in 400 µl Hepes-rhodamine buffer (5 µM rhodamine 6G). The cells were incubated in a 30 ºC water bath for 2 hrs allowing the cells to load rhodamine 6G by passive diffusion. 600 µl Hepes was added to the cells and centrifuged at14,000 RPM. The cells were resuspended in 400 µl Hepes containing 1 mM glucose without rhodamine 6G and incubated at 30 ºC for 30 min facilitating efflux before chilling them on ice to terminate

transport. The cells were then pelleted by centrifugation at 14,00 RPM. The pellet was resuspended in 300 µl Hepes buffer and transferred to a tube for FACS analysis. The fluorescence of rhodamine 6G was measured using a Becton-Dickinson FACSort (Franklin Lakes, NJ). The excitation wavelength was 488nm and emission wavelength was 585 nm. The resulting date was analyzed using a Cell Quest program (BD Biosciences, San Jose, CA).

I. Plasma Membrane Isolation and Quantification

Isolation of yeast plasma membrane

Two days prior to isolating plasma membrane 5 ml YPD medium was inoculated with desired double copy yeast strain and grown overnight at 30 ºC with shaking. 15 hrs prior to harvest 750 ml YPD broth was inoculated with 0.25 X 10^5 cells from initial starter culture and incubated at 30 ºC with vigorous shaking. Just prior to harvest 1 mM phenylmethyl sulfonyl fluoride (PMSF) was added to the bulk cultures. The cultures were incubated for an additional 20 min at 4 ºC. The cells were harvested by centrifugation at 3,500 RPM for 12 min at 4 ºC in a Sorval centrifuge using a GS-3 rotor. The supernatant was discarded and the pellet was resuspended in 5 ml sterile reverse osmosis water (RO-H_2O). The resuspension was transferred to a 40 ml Okaridge tube and centrifuged at 3,500 RPM for 12 min at 4 ºC in a Sorval centrifuge using a GS-3 rotor. The supernatant was discarded and the weight of the wet pellet was determined. The pellet was resuspended in 2X volume of the homogenization buffer, pH 7.5 (5 ml 1 mM Tris-Cl, 0.5 ml of 0.5M EDTA and 93.5 ml RO-H_2O). The following protease inhibitors (Sigma, St.

Louis,MO) are added to the buffer; aprotinin (10 µl/ml), TPCK/TPLC (10 mg/ml stock, 10 µl/ml), leupeptin (1 mg/ml stock, 1 µl/ml), PMSF (14.7 mg/ml stock, 10 ul/ml) and pepstatin (1 mg/ml stock, 1 µl/ml). The resuspended cells were then subjected mechanical lysis in a bead beater containing 10 ml of 0.5 mm acid washed glass beads. The cells were disrupted by 5 cycles of 30 sec beating followed by 30 sec of cooling. The lysate was collected in an Okaridge tube. The process was repeated for another two cycles of 30 sec beating and 30 sec resting by addition of homogenization buffer. The remaining lysate was also added to the Okaridge tube. The lysed cell walls and the unlysed cells were pelleted by centrifuging the sample at 7,500 RPM for 6 min at 4 ºC in a Sorval centrifuge using a SS-34 rotor. The supernatant was transferred to a pre-chilled open top polyclear 16 X 76 ultracentrifuge tubes and filled to the top with homogenization buffer containing protease inhibitors and subsequently centrifuged at 40,000 RPM for 1 hr at 4 ºC.in a Beckman Ultracentrifuge using a Ti50 rotor. The supernatant was discarded and the pellet containing the crude membrane preparation was suspended in 2-3 ml of resuspension buffer containing the following protease inhibitors; aprotinin (10 µl/ml), TPCK/TPLC (10 mg/ml stock, 10 µl/ml), leupeptin (1 mg/ml stock, 1µl/ml), PMSF (14.7 mg/ml stock, 10 ul/ml) and pepstatin (1 mg/ml stock, 1 µl/ml). The buffer with the pellet was transferred to a pre-chilled Dounce homogenizer and the plunger was used to completely resuspend the pellet. A sucrose gradient was prepared in a 25 X 89 mm centrifuge tube by layering 17.5 ml of 43.5 % sucrose on 17.5 ml of 53.5 % sucrose solution. The resuspended crude membrane was layered on a sucrose gradient and centrifuged in a SW-27 swinging bucket rotor at 25,000 RPM at 4 ºC for 5 hrs. Purified plasma membrane trapped at the interface of the sucrose gradient was removed

with a transfer pipette and split into two 16 X 17 ultracentrifuge tubes. The tubes were filled with resuspension buffer and centrifuged in a Backman Ultracentrifuge at 40,000 RPM at 4 ºC for 1 hr using a Ti50 rotor. After centrifugation the supernatant was discarded and the pellet containing purified plasma membrane was resuspended in 300-500 ul of resuspension buffer. 50 µl quantity of the membrane preparation was aliquoted into1.5 ml microfuge tubes. The tubes were stored at -70 ºC.

Plasma membrane protein quantification

Pierce BCA Protein Assay Kit (Thermo Scientific, Rockford, IL) was used to determine the protein concentration of the purified plasma membrane vesicles. The protein concentration was determined by using a standard curve. The standard curve was obtained from a series of tubes containing various amounts of BSA (Thermo Scientific, Rockford, IL). The volume was made up to 100 µl with water. Color was developed by adding 2 ml of A+B solution and incubating the tubes at 37 °C for 30 min. A_{562} vs BSA 2 mg/ml was plotted on the graph to obtain a standard curve.

Western Blotting

30 µg of plasma membrane protein was loaded onto a 7 % Tris acetate gel (Invitrogen, Carlsbad, CA) and run at 150 V until the dye ran off the gel. The resolved proteins were electrophoretically transferred to a nitrocellulose filter in transfer buffer (Invitrogen, Carlsbad, CA) using the X Cell II- Mini Cell apparatus (Novex, San Diego, CA). Protein transfer onto the nitrocellulose filter was confirmed using Ponceau S stain. To reduce nonspecific binding, the nitrocellulose filter was incubated in 10 ml of NF-

PBST (20 ml of 10XPBS, 2 ml of 10% tween, 5 g nonfat milk and 178 ml reverse osmosis water) for 30 min at room temperature. 1:1000 dilution of Pdr5 and Pma1 antibody in PBST was added to the membrane and incubated overnight at 4 °C. The next morning the nitrocellulose filter was washed thrice in 10 ml PBST (20 ml of 10X PBS, 2 ml of 10 % tween, and 178 ml reverse osmosis water). After washing, the membrane was incubated in 10 ml of secondary antibody (1:5000 in NF-PBST) for 2 hrs at RT. The membrane is then washed thrice with 10 ml PBST to remove unbound antibody. The nitrocellulose membrane was then treated with a chemiluminescence reagent (Invitrogen, Carlsbad, CA). The Pdr5 and Pma1 bands were visualized by exposing the membrane to a film for 30 sec to 1 min.

J. Plasma Membrane Analysis

ATPase assay

ATPase activity of Pdr5p was measured using a colorimetric reaction, by quantifying the amount of P_i (organic phosphate) released upon hydrolysis of ATP. 12 µg of plasma membrane and 50 µl assay buffer (100mM MOPS (pH7.0), 50 mM KCl, 5 mM $NaNO_3$, 2 mM EGTA (pH7.0), 2 mM DTT and 10 mM $MgCl_2$) were added to a pre-chilled 13 X 100 mm glass tube. The sample was made up to 95 µl with sterile water. The reaction was initiated by adding 4 µl of 3 mM adenosine 5'-triphosphate (ATP) and incubating the tube at 35 °C for 8 min. The reaction was terminated by addition of 100 µl of 2.5 % sodium dodecylsulfate (SDS). Color was developed by addition of 400 µl P_i reagent (1% ammonium molybdate in 2.5 N sulfuric acid with 0.014 % antimony

potassium tartarate), 500 µl sterile reverse osmosis water, 200 µl of 1 % ascorbic acid, and incubation for 10 min at RT. The absorbance was read at 880 nm and the ATPase activity of the sample was calculated.

K. Isolation of Second-site Suppressor Mutation in PDR5

Clo resistant (clo^r) suppressors of E1013A by plating $1X10^6$ cells on medium containing 7.5 µM clotrimazole and incubating them for 5 days at 30 ºC. Only the cells that acquired second site mutation that restored drug resistance grew on clotrimazole. The experimental strategy for determining whether the suppressor mutation is in PDR5 or elsewhere in the genome is illustrated in Figure 2.

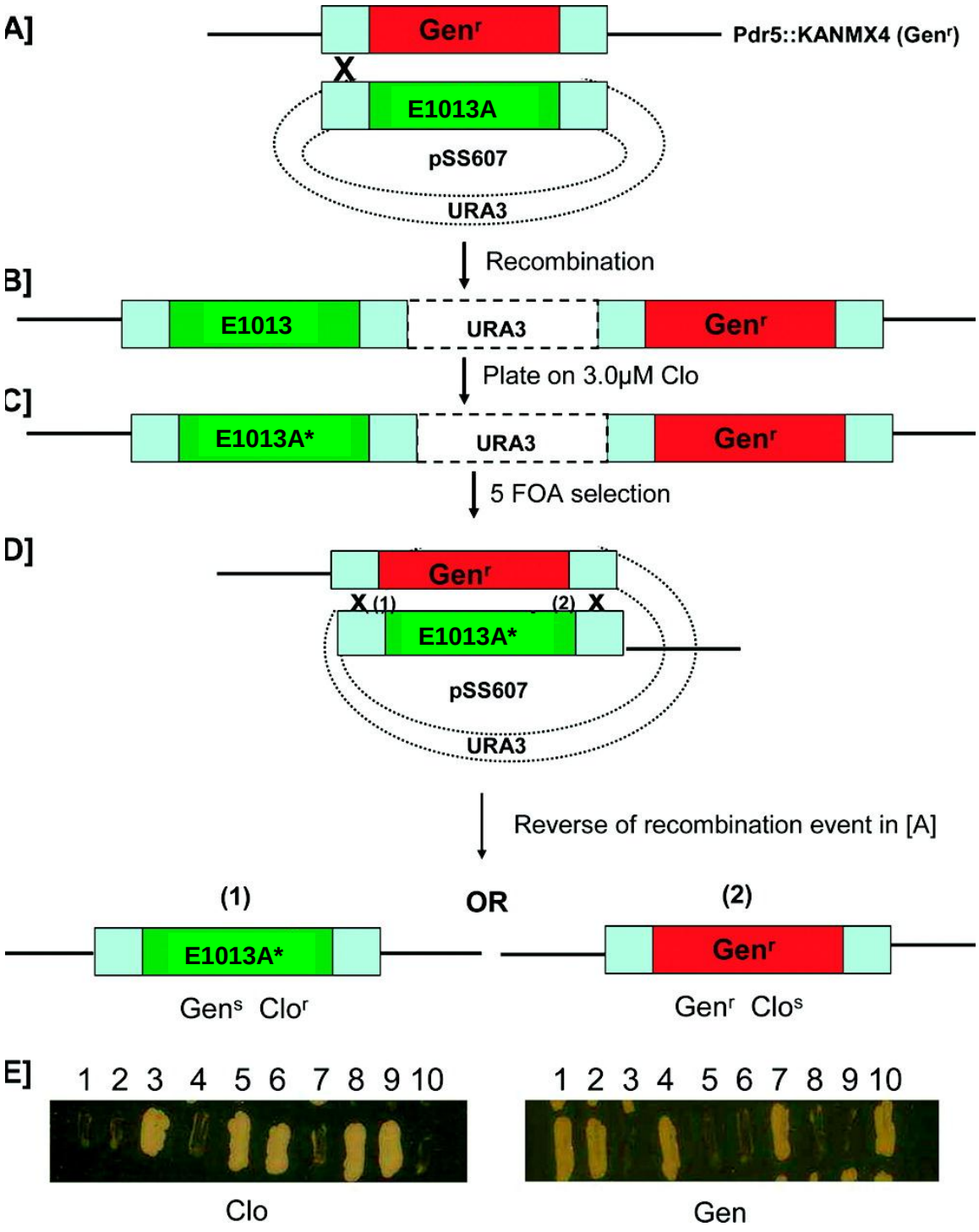

FIGURE 2: Experimental strategy designed to determine whether a suppressor is due to a second-site mutation in *pdr5*$_{S558Y}$. *A, B* Suppressors were isolated as chromosomal mutations in JG2011 which has two *PDR5* cassettes. The first has the coding sequence replaced with *KANMX4* but retains the upstream and downstream flanking regions. This is separated by plasmid sequences including the selectable marker *URA3* from a second copy of *PDR5* containing E1013A. *C,* In this illustration, it is

assumed that the new mutation (*) lies in E1013A rather than in a second gene (the case for all of the mutants recovered as S558Y suppressors). *D,* Loss of the plasmid sequences containing *URA3* and one of two *PDR5* cassettes (either *pdr5::KANMX4* or $pdr5_{E1013A}$) occurs by homologous recombination. These events result in *Ura-* colonies that are selected on plates containing 1 mg / ml 5-FOA. These are tested on gen (200 mg/l) and clo-containing medium (7.5 μM). *E,* If the suppressor is attributable to a second mutation in the E1013A-bearing copy, $clo^r\ gen^s$,and $clo^s\ gen^r$ recombinants will be recovered as shown.

RESULTS

PART I: Mapping the signaling interface in Pdr5

The drug efflux cycle in an ABC transporter involves the binding of the drug to the TMDs and ATP to the NBDs. Hydrolysis of ATP triggers a conformational change at the TMDs resulting in drug efflux (Linton *et al.*, 2004). Biochemical and genetic data along with X-ray structure of Sav1866 (Locher *et al.*, 2006) suggest a transition interface between the TMDs & NBDs in which the Q loop of one NBD makes contact with TMDs via the intercellular loops. Previously, the Q loop was implicated in communication between the TMDs and the NBDs in several ABC transporters (Locher *et al.*, 2006, Tampe *et al.*, 2009). Part I aims at understanding the communication between the TMDs and NBDs in Pdr5 by identifying key residues that would map the signal interface.

Isolation and sequence analysis of mutants that suppress the clotrimazole hypersensitivity of S558Y.

The strategy for isolating independent suppressors of S558Y clotimazole (clo) hypersensitivity has been previously described (Sauna *et al*., 2008). In that study, nine suppressors of S558Y were isolated. The experimental strategy for determining whether a suppressor results from a second mutation in *PDR5* or from a mutation elsewhere in

the genome is illustrated in Figure 2. The recovery of Gen^r Clo^s and Gen^s Clo^r segregants provided qualitative proof that the responsible mutation arose in *PDR5*. In all cases, the suppressor phenotypes were attributable to a second mutation in the *PDR5* gene.

The *PDR5* coding region was recovered and the DNA was sequenced to determine the location of the mutations (Table 1). All of the mutants contained the original S558Y mutation plus a single additional alteration. A schematic representation of the mutants is shown in Figure 3 as a 2-D topological map of Pdr5. Of the nine mutants analyzed, seven were in either the N-terminal NBD or ICL1. One mutation is an E244G substitution. When alignment of Pdr5 with other transporters was carried out (Figure 4, 5), the Glu-244 residue was found to be completely conserved in the Pdr5 fungal subfamily of multidrug transporters and to be a replacement for the Gln in the canonical Q-loop of other ABC transporters (Xia *et al*., 2010).

Table 1: Location of suppressor mutations

Residue alteration	Location	No. found	Comments
N242K	NBD1 near the Q loop (between Walker A and B)	1	Sauna *et al*., 2008
E244G	Defines Q-loop	1	Completely conserved residue equivalent of Q951G in NBD2
D246Δ	NBD1 Q loop	2	Deletion of a triplet codon of a highly conserved residue
S597X	ICL1	3	2 alleles are S597I; 1 allele is S597T
M679L	TMH5	1	
G1233D	ECL4 between TMH7 and TMH8	1	

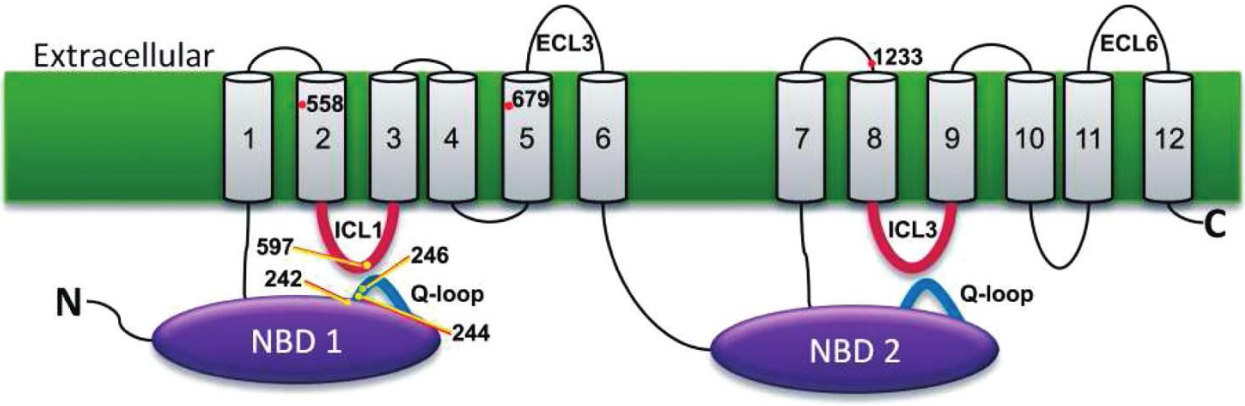

Figure 3. Location of suppressor mutations in Pdr5. Mutations that suppress S558Y (TMH2) are shown on a 2-D topological diagram of Pdr5.

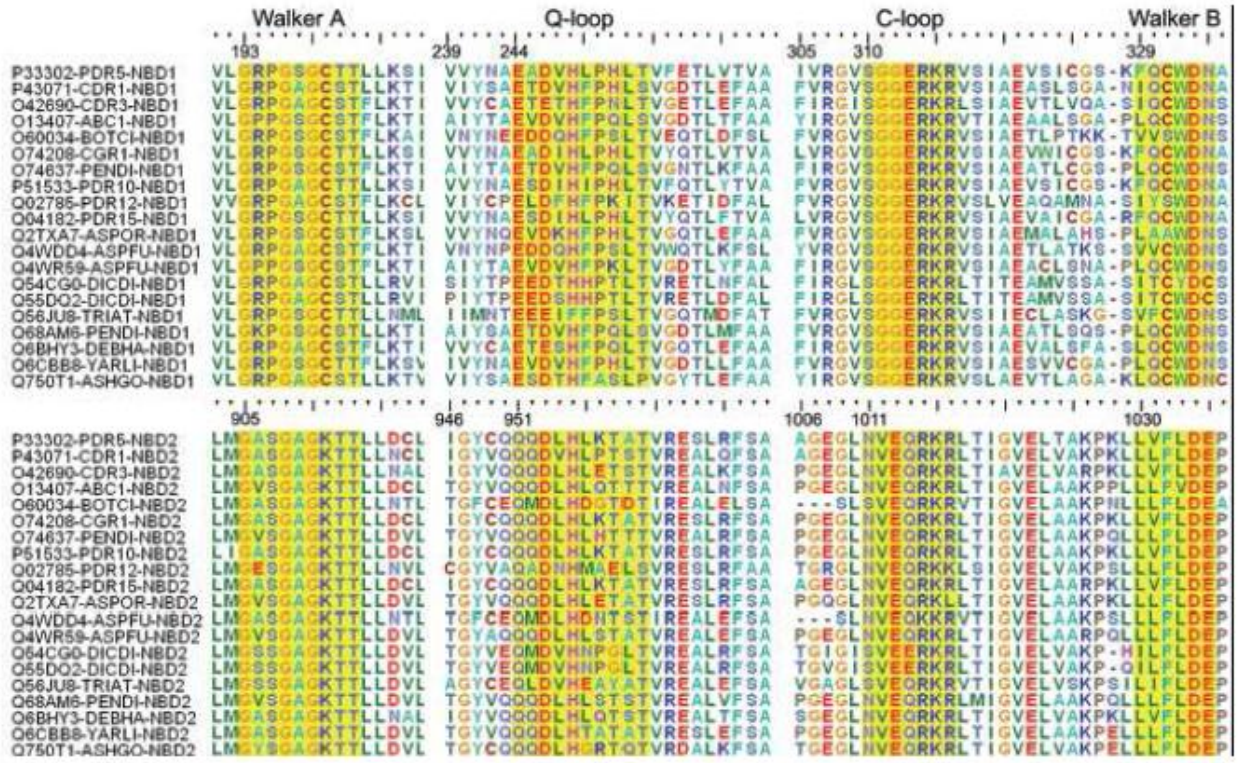

Figure 4: An alignment of 20 members of the Pdr5 subfamily of fungal ABC transporters. The atypical ATP-binding site and surrounding nucleotides including Gln-244 are composed of the Walker A, Walker B, and Q-loop regions of the N-terminal NBD and the signature region of the other NBD. These sequences are shown for this subfamily in the top-half of the alignment. The equivalent sequences for the canonical site including Glu-951 are shown in the bottom half.

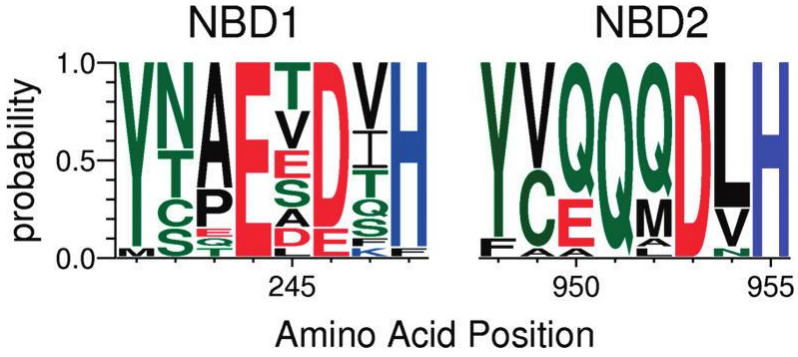

Figure5: The Q-loop region motif. The figure shows the deviant portion of the N-terminal NBD (left side) and the canonical counterpart from NBD2 (right side). A protein sequence logo depicting the conservation of residues in and around the Q-loops of

NBDs 1 and 2 was constructed from the multiple sequence alignment of Pdr5p as described previously (Kim *et al.*, 2006).The height of each letter represents the probability of the residue occuring at that position in the alignment. The colors signify the chemistry of the amino acids: red, acidic; blue, basic; black, hydrophobic; green, polar.

With this information, a conserved motif was identified by comparing regions in the 2 NBDs. (Figure 5) The motif is Y /F, Sp, X, E, X, D /E, X, H, where Sp is a small polar residue (N, S, T, or C) and X is not conserved. Three mutations appeared in two of the conserved residues. There were three independent alterations at residue Ser-597 in ICL1 (two were S597I, one was S597T). The remaining mutants were an M679L substitution in TMH5 and the G1233D mutation in ECL4 connecting TMH7 and 8. No mutations in NBD-2 were recovered. It is striking that seven of the nine independently isolated suppressor mutants had an alteration near or at the Q-loop and in ICL1. Thus, the location of these mutants on both sides of the interface lends functional evidence to previous structural and crosslinking studies, which suggested that at least one signaling interface runs from the NBD through ICLs and into the TMDs. This arrangement, although reminiscent of the Sav1866 transporter, which functions as a homodimer, is strikingly different in one crucial feature. The crystallographic data from Sav1866 suggests an interface with a criss-cross or trans arrangement in which the Q-loop of 1 monomer interacts with the ICL of the other. Evidence for a similar arrangement is found in eukaryotic transporters Tap and P-gp (Linton, *et al*., 2007, Tampe, *et al*., 2009). The results, however, strongly suggest that the cis arrangement is physiologically relevant in Pdr5.

The drug phenotypes of the suppressor mutants**.**

The relative resistance of the suppressor mutants to cyh and clo were evaluated using an IC-50 assay (Figure 6A and B). Although the suppressors were selected on clo-containing medium, all of them restored significant cyh resistance as well. Furthermore, none of the mutants were as resistant as the WT control to either drug. Finally, the curves generated for each mutant were similar. In fact, several of the clo plots completely overlapped; making it appear-erroneously-as though fewer strains were tested on this drug. Thus, all of the mutants had IC_{50}s for clo of ~4.0 – 8.0 μM and IC_{50}s for cyh of ~ 3.5 – 4.0 μM. These values represent a significant increase in resistance when compared to the values for S558Y, which are 1.1 μM and 0.4 μM for clo and cyh, respectively.

Because the E244G mutation is the subject of a detailed study, The E244G, S558Y suppressor mutation was recreated in pSS607 and compared the clo resistance of the plasmid-borne suppressor mutation to the chromosomal equivalent (Figure 6C). The IC_{50}s of the chromosomal and plasmid E244G, S558Y suppressor were, within experimental error, indistinguishable. In each case, they showed an ~8-fold increase in clo resistance when compared to S558Y. Although all of the suppressor mutations are interesting and most lie in a general interface suggested by structural and crosslinking studies, E244G was further examined.

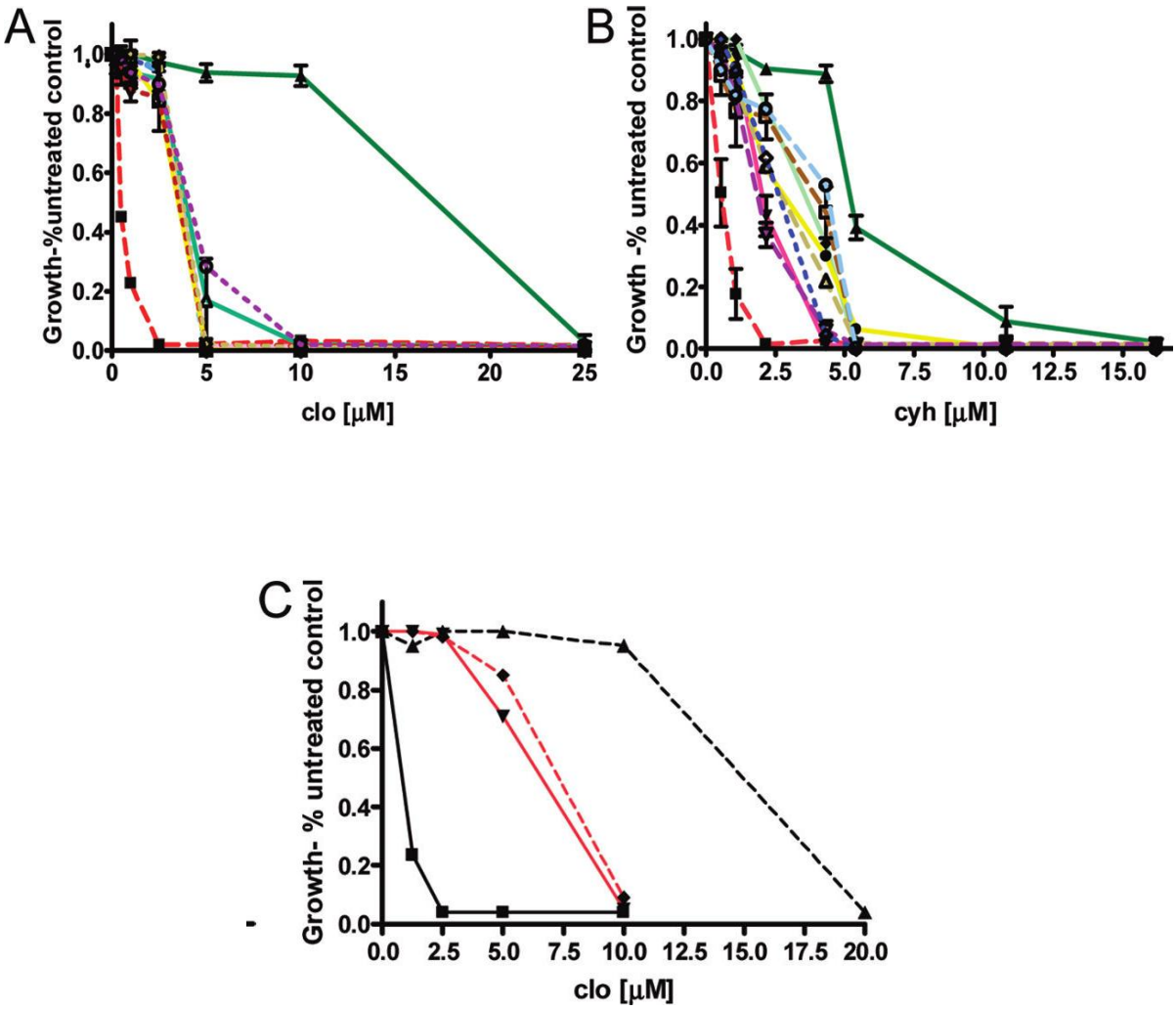

Figure 6: Quantitative analysis of drug resistance in suppressor mutants. Strains were inoculated into 2 ml YPD containing *A*, clo (1.25-25.0 μM) or *B*, cyh (0.25-21.6 μM) at an initial cell concentration of 25,000 cells /ml. Cultures were grown in a shaking bath at 30° C for 48 hr prior to determining the cell concentration using A_{600}. Drug-free cultures of each strain served as a control. In each panel ▲is WT, ■ is S558Y. Because many of the mutant curves superimpose, no attempt was made to distinguish the individual mutants. *C*, The E244G, S558Y double mutation was made in pSS607 (♦) for comparison with the original chromosomal suppressor mutation (▼).

<u>The effect of NBD mutations in a S558 (otherwise WT) background</u>**.**

The effect of E244G mutation on drug resistance was evaluated in an S558 (otherwise WT) background. The Q-loop is thought to facilitate communication between the ATP-binding site and the ICLs (Veen *et al*., 2009). As a means of comparison, the corresponding mutation in NBD2; Q951G was also constructed. The colloidal-blue gel scan and Western blot were prepared from strains containing double copies of WT and these mutants. The levels of Pdr5p in purified plasma membrane vesicles were similar (Figure 7A). The relative cyh and clo resistance of these strains and the double mutant E244G, Q951G, along with isogenic negative and positive controls were determined (Figure 7B and C). Compared to the WT, E224G showed significant cyh sensitivity but its resistance to clo was only slightly lower (1.3-fold reduction in IC_{50}). The phenotype of the corresponding NBD2 mutant, Q951G, was similar. This mutant was ~2-fold more sensitive to cyh than was the WT. The Q951G strain, however, exhibited significantly greater clo hypersensitivity (3.4-fold) than did the E244G mutant. Compared to either S558Y or Δ*pdr5*, however, the phenotypes of these mutants were quite similar. Therefore, E244G is not a gain-of-function mutation in a nonessential residue and is required for WT levels of drug resistance.

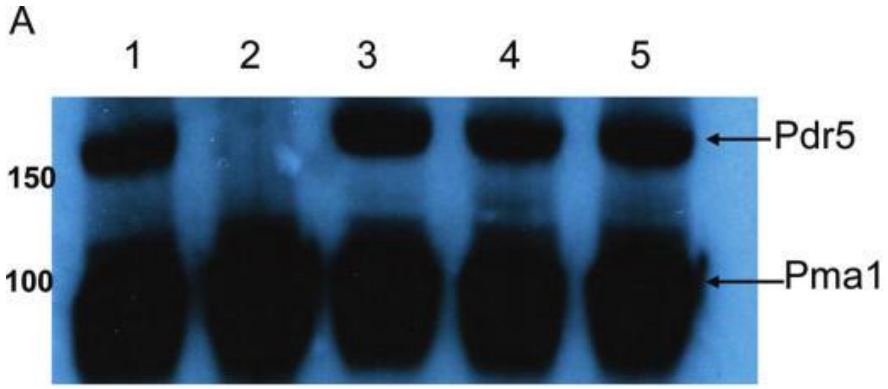

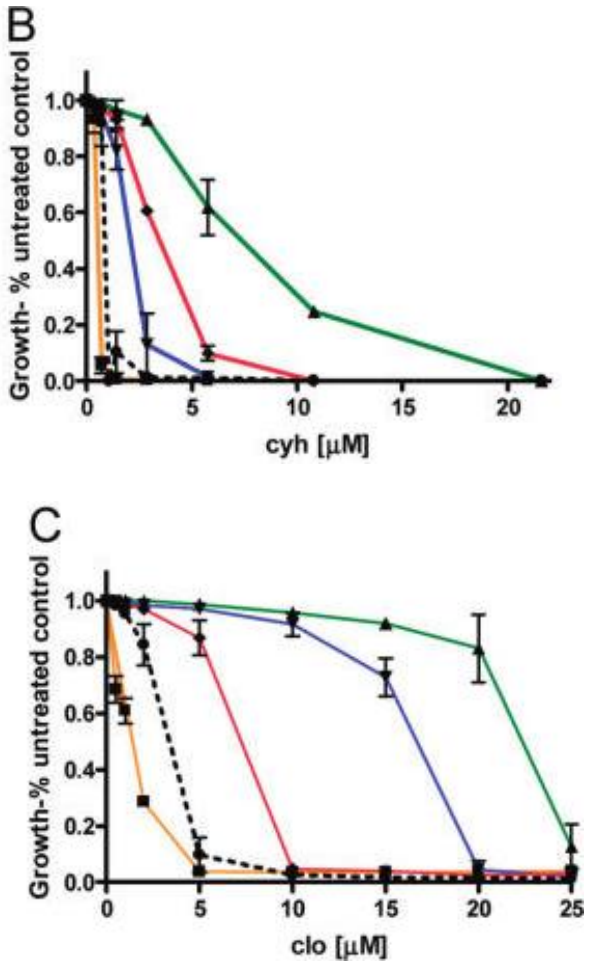

Figure 7: Phenotypic features of the E244G and Q951G mutations. *A*, Colloidal-blue stained gel and *B*, an immunoblot of purified plasma membrane PM vesicles prepared from various strains of yeast. A sample of solubilized protein was divided into two, 20 μg portions and these were used for a colloidal-blue stained gel and an immunoblot. Conditions for gel electrophoresis and Immunoblotting were previously described (Sauna *et al*., 2008). The lanes are as follows: lane 1, molecular weight markers; lane 2, WT; lane 3, *Δpdr5;* lane 4, E244G; lane 5, Q951G; lane 6, E244G, Q951G; Quantitative analysis of *C*, cyh and *D*, clo resistance. Cultures containing drug were set up and grown as described (Sauna *et al*., 2008). The plots and statistical analysis were carried out using GraphPad Prism software. The figures show the mean values of three independent experiments and the error bars represent the S.D. In these panels the strains are designated as follows: ▲is WT, ■ is S558Y, ▼is E244G, ♦ is Q951G, ●(---) is E244G, Q951G.

Double-mutant analysis: redundancy of Q-loop function during ATP hydrolysis.

The single-mutant analysis led to several important observations. First, although E244G was a dramatic alteration in a highly conserved residue, it created only mild drug hypersensitivity. The same was true for Q951G in the canonical ATP-binding domain. E244G appeared more sensitive to cyh than clo, and Q951G appeared somewhat more sensitive to clo than cyh. All, however, were considerably more resistant than S558Y. The relatively mild loss in the drug resistance of the single mutants suggested that there might be functional overlap between the corresponding region in NBD-2. Essentially, then, only Glu-244 or Gln-951 is actually required for Pdr5 to mediate a significant portion of its drug resistance to cyh or clo.

To further investigate the possible functional overlap between the 2 Q-loops, a E244G, Q951G double mutant was constructed. The drug sensitivity of the double mutant was compared to WT. They were quantitatively tested for their cyh and clo drug resistance. The results for E244G, Q951G are shown in Figure 7B (cyh) and 7C (clo). The IC_{50} values for cyh were calculated. It was found that the difference in sensitivity relative to the WT strain was 17.2 for S558Y, 2.60 for E244G, 1.9 for Q951G, and 6.81 for E244G, Q951G. If the Q-regions were functioning independently and the 2 mutants were partially impaired in biochemical function, the double mutant would show simple additivity and thus be 4.50-fold more sensitive. The observed value of 6.81-fold was significantly greater than we expected. These initial results thus suggested that at least some functional redundancy exists between the 2 Q-loops during ATP hydrolysis. Results with clo also showed a similar pattern. In this set of experiments, the difference

between WT (22.5 μM) and E244G (17.5 μM) was only 1.3-fold. The Q951G strain had an IC_{50} of 6.78 μM, a 3.40-fold difference. Thus, the expectation for the double mutant based on simple additivity is a difference from the WT strain of 4.7-fold. In fact, the E244G, Q951G mutant was 7.7-fold more sensitive than the WT.

The large difference in drug sensitivity between the single and double mutants was also observed qualitatively for 1.5 mM and 3.0 mM chloramphenicol, a moderately strong transport substrate used in whole-cell and vesicle transport assays (Sauna *et al.*, 2007, Golin *et al.*, 1994, Golin *et al.*, 2003). The single E244G and Q951G mutants were all qualitatively similar to WT. The E244G, Q951G double mutant was phenotypically very hypersensitive and similar to S558Y (Figure 7B, C).

It was theoretically possible that the profound drug hypersensitivity observed with the double mutant was not entirely attributable to the combined E244G, Q951G alterations in Pdr5, but rather to an additional mutation in the genome that occurred spontaneously. Two additional, independent E244G, Q951G transformants were tested. The drug hypersensitivity was indistinguishable from that seen with the original double mutant. Thus, when analyzed together for their resistance to clo, all three E244G, Q951G independently constructed strains had identical minimum inhibitory concentrations of 5 μM and IC_{50}s of ~2.9 μM.

The effect of Q-region mutations on NTPase activity.

The effect of Q-loop mutations on ATP hydrolysis has not been investigated extensively, but two studies with ABC transporters suggest that these alterations do not affect catalysis. For instance, although the bacterial MsbA transporter Q-loop residue appears to be required for the proper conformational signaling change during ATP hydrolysis, a Q-to-C mutation does not affect ATPase activity per se (Dalmas *et al.,* 2005). Analogous results were found with P-gp *(*Urbatsch *et al.,* 2000*).* In reporting on a study that used FRET (Forster resonance energy transfer) Rai *et al*., (2008) suggested a role for the equivalent Cdr1 residue (Glu-237) in coordinating the Mg ion during ATP hydrolysis, but this study was carried out with a single, purified NBD and did not look directly at ATPase activity or determine a drug phenotype.

The Pdr5-ATPase activity of E244G and Q951G was evaluated along with S558Y, E244G (Figure 8A and 8B). For comparison, V_{max} and K_m values for S558Y were also included that were previously published (Sauna *et al.,* 2008). The average (n=3) WT value of ~220 nmol/min/mg was in the range reported previously for such double-copy strains: ~179-275 nmol/min/mg (Sauna *et al.,* 2008). This was ~4 fold higher than the V_{max} of E244G or Q951G, which were each ~50–60 nmol/min/mg (Figure 8B). It is particularly striking that mutation of the canonical Gln-951 residue and the deviant Glu-244 had an equivalent ATPase deficiency as well as similar drug hypersensitivity. Although the reduction in ATPase activity of the Q-loop mutants was

clear, significant activity remained. Therefore, it is highly unlikely that these residues are required for the reaction chemistry of NTP hydrolysis.

There was little or no difference in the observed K_ms (Figure 8C). This suggests that none of the mutants has a significant effect on ATP-binding. Data from our previous work (Sauna *et al.,* 2008*)* and the present study strongly suggest that Pdr5 has poor coupling of ATP hydrolysis to drug transport. For instance, E244G restores considerable drug resistance to S558Y, yet they did not increase the basal level of ATPase activity. Furthermore, there was a relatively poor correlation between the ATPase activity of the E244Gand Q951G mutants and the IC_{50} data for cyh. This can be seen in Table 3, which summarizes the important phenotypes for the mutants. These observations support the contention of Ernst *et al.,* (2008, 2010) that much of the basal ATPase activity is uncoupled from transport - at least for the substrates that we employ.

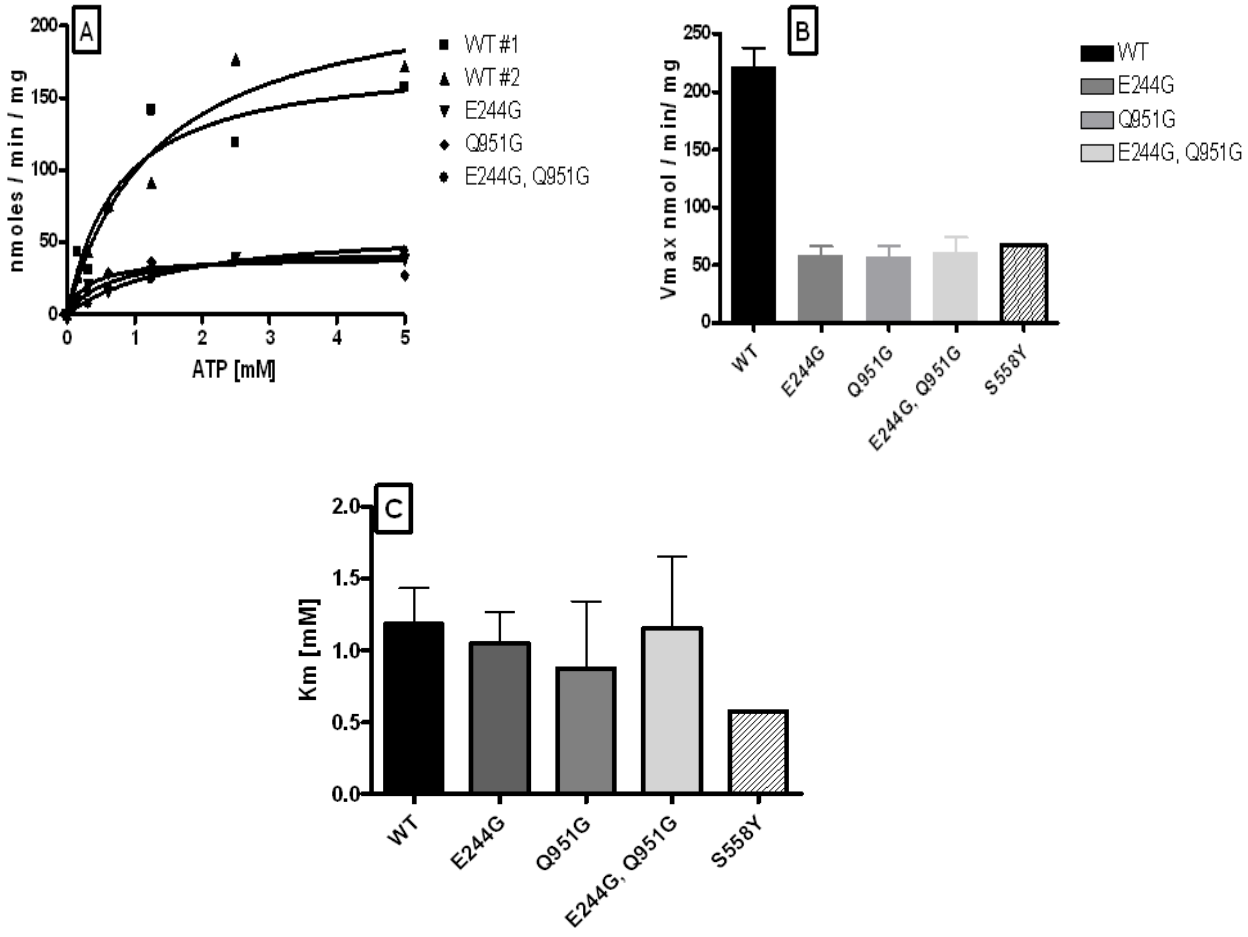

Figure 8: The ATPase activity of single and double mutants. *A,* ATPase assays were conducted with purified plasma membrane vesicles recovered from strains bearing a double copy of the WT, single or double mutants. A representative experiment is shown for each strain. The data for S558Y were previously reported and serve as a reference (Sauna *et al.*, 2008). ATPase activity was determined as previously described in Golin et al., 2007 using 12 µg purified plasma membrane incubated for 8 min at 35°C before terminating the reaction with 2.5% SDS. The small amount (< 10%) of non-specific activity found in the *Δpdr5* strain (R-1) is subtracted when calculating activity. Data were analyzed using GraphPad Prism software. The strains are represented as follows: ■ is WT, ▲is E244G, ▼is Q951G, + is S558Y, E244G, * is S558Y and ♦ is E244G, Q951G *B,* and *C,* The kinetic parameters of ATPase activity in WT and mutant plasma membrane vesicles. The values represent at least 3 independent experiments carried out with two (Q951G) or three different plasma membrane vesicle preparations of each strain.

Table 2: Summary of important phenotypic characteristics

Residue alteration	IC_{50} (μM cyh)	Δ[1]	IC_{50} (μM clo)	Δ	V_{max} (ATPase)	Δ
WT	7.50		22.5		222	
S558Y	0.43	17.4	1.11	20.3	74.8[2]	2.9
S558Y, N242K[2]	4.10	1.8	Not done		88.9	2.5
S558Y, E244G	3.75	2.0	8.25	2.7	82.4	2.7
N242K	3.75	2.0	15.0	1.5	144	1.6
E244G	2.93	2.6	17.5	1.3	58.5	3.8
Q951G	3.90	1.9	6.78	3.4	57.3	3.7
E244G, Q951G	1.10	6.8	2.92	7.7	61.0	3.6

In light of the equivalence of the deviant and canonical Q-loop residues and the greater than additive hypersensitivity of the E244G, Q951G strain, double mutant was expected at least show an additive ATPase deficiency. If this were the case, the V_{max} of the double mutant would be ~25 nmol/min/mg, a value that would be quite noticeable with our assay conditions. Significantly, the ATPase of the E244G, Q951G double-mutant strain was no lower than that of the single mutants, even though the difference in clo drug sensitivity between this strain and E244G was greater than 5-fold. This observation has several important implications, the most significant of which is that the severe transport deficiency in the double mutant is caused by something other than a further loss of ATP hydrolysis.

Pdr5 has a significant GTPase activity that is capable of fueling transport and is approximately 0.4 that of its ATPase counterpart (Golin *et al., 2007*). Data presented in Figure 9 demonstrate that both E244G and E244G, Q951G had a V_{max} for the WT was only ~1.5- to 2-fold higher than that of the mutants. The reduction in GTPase activity of the mutants was therefore significantly less than that observed for ATPase activity. Furthermore, the plots of E244G and E244G, Q951G activity versus GTP concentration are indistinguishable. Thus, the sharp reduction in drug resistance observed for E244G, Q951G could not be attributed to a further loss of NTPase function.

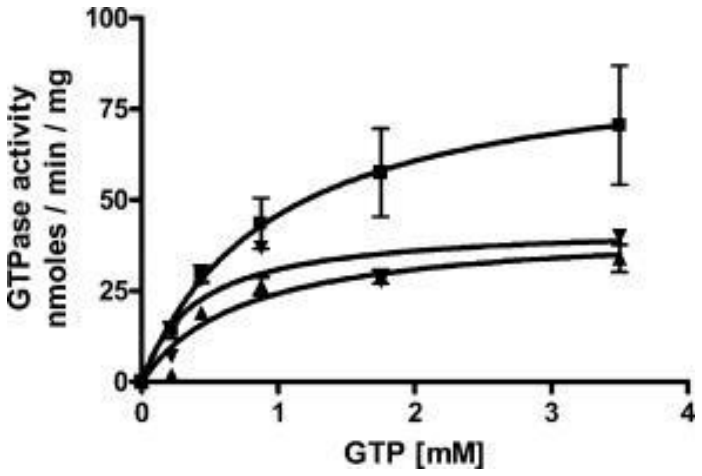

Figure 9: The GTPase activity of WT, E244G, and E244G, Q951G. The assay for GTPase activity is identical to the one used to measure ATP hydrolysis except that 16 μg of plasma membrane protein was used in each reaction GTPase activity of WT (■), E244G (▲), and E244G, Q951G (▼) were compared. Plots are the average of three independent experiments from three independent plasma membrane vesicle preparations of each strain (n=3).

PART II: Deviant ATP Binding Site of Pdr5: Evidence for a Novel Functional Role

Part I of the results demonstrates that the deviant and the canonical Q-loop are functionally equivalent. The data also suggests an interdomain communication between deviant NBD and TMD-1 via the deviant Q-loop and ICL-1. Since a signal interface is passing through the deviant NDB, it indicated that the deviant site plays an important role in Pdr5 function. The role of the deviant ATP binding site remains largely unexplored among ABC transporters. Part II aims at understanding the importance of the deviant ATP binding site in Pdr5. by biochemically analyzing deviant signature and Walker A residues.

The deviant signature motif residue Glu-1013 is not equivalent to its canonical counterpart Gly-312

G312A and E1013A mutations were constructed in the completely conserved signature regions of the canonical and deviant ATP-binding sites. Western blotting was performed (Figure 10A) to verify the presence of Pdr5 in purified plasma membranes. After introducing these mutations into the Δ*pdr5* strain R-1, their resistance to clo and cyh (Figure 10B, 10C) and their capacity to transport R6G (Figure 10D) was evaluated. With regard to clo resistance, the canonical site mutant, G312A is as sensitive to clo as the Δ*pdr5* control. The minimum inhibitory concentration (MIC) is less than 0.5 μM. This is not a surprising result as it is well established that conserved signature residues are essential in ABC transporters. The E1013A mutation however is not phenotypically

null although it is hypersensitive to clo. The MIC of 4 μM is about 3 times less than WT. Next, the sensitivity of the mutants to cyh was tested (Figure 10C). G312A, like its clo phenotype, was as sensitive as Δ*pdr5*.E1013A was hypersensitive to cyh with MIC of 1μM which is about 7 times less than WT. It is interesting to note that E1013A is more sensitive to cyh than clo. However, the deviant signature residue mutant, E1013A, retains some amount of drug resistance when compared with the canonical signature mutant, G312A. The R6G transport data demonstrate an even more striking disparity between the signature residues. These results (Figure 10D) again demonstrate the severity of G312A which is nearly as impaired in R6G as Δ*pdr5.* The median retained fluorescence for these strains is 1025 and 1421 respectively. However, E1013A mutant shows a strong R6G transport with a low fluorescence (44.25) that is nearly WT (11.24). These results clearly demonstrate that the canonical anddeviant signature residues are not functionally equivalent.

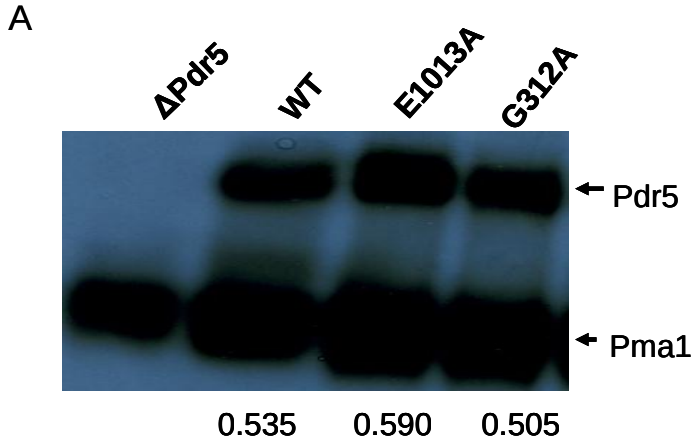

B

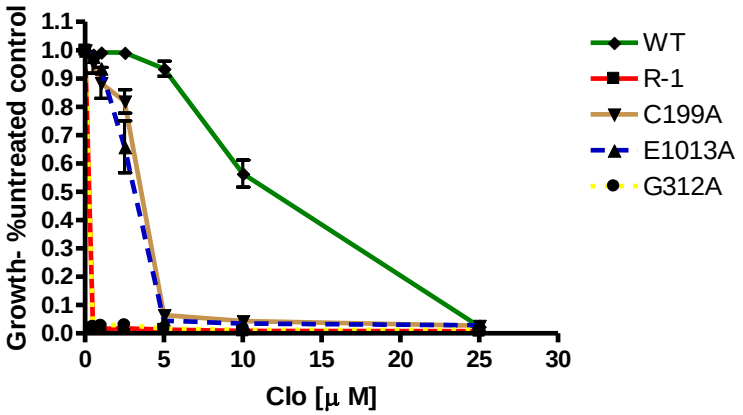
Growth- %untreated control
1.1
1.0
0.9
0.8
0.7
0.6
0.5
0.4
0.3
0.2
0.1
0.0
0
5
10
15
20
25
30
Clo [μ M]
WT
R-1
C199A
E1013A
G312A

C

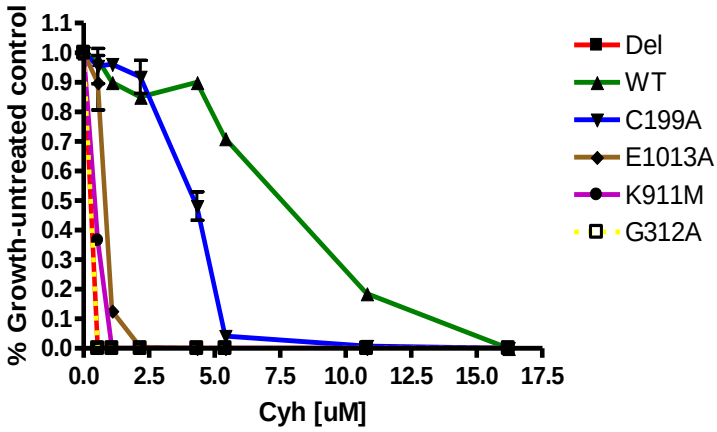
% Growth-untreated control
1.1
1.0
0.9
0.8
0.7
0.6
0.5
0.4
0.3
0.2
0.1
0.0
0.0
2.5
5.0
7.5
10.0
12.5
15.0
17.5
Cyh [uM]
Del
WT
C199A
E1013A
K911M
G312A

D

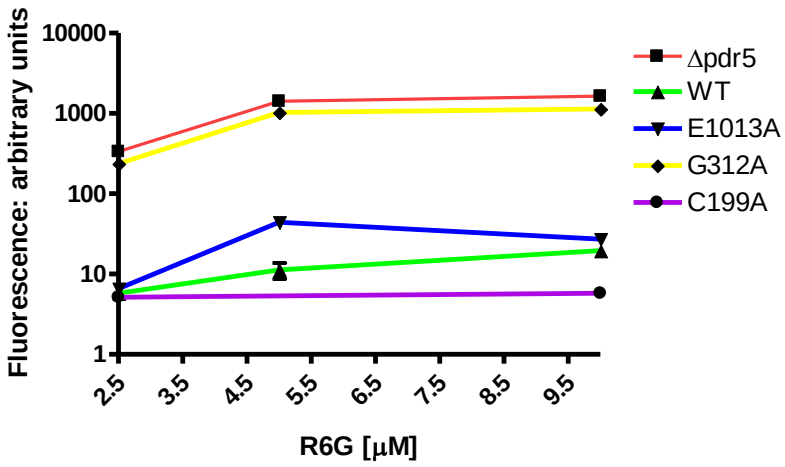
Fluorescence: arbitrary units
10000
1000
100
10
1
2.5
3.5
4.5
5.5
6.5
7.5
8.5
9.5
R6G [μM]
Δpdr5
WT
E1013A
G312A
C199A

Figure 10: Characterization of E1013A and G312A. *A,* an immunoblot of purified plasma membrane (PM) vesicles prepared from various strains of yeast. Samples containing 20 μg of PM vesicles protein were solubilized in SDS─PAGE for 30 min at 37 °C. The samples were subjected to gel electrophoresis and immunoblotting. The number in each lane is the ratio of Pdr5 to Pma1 and was determined using image J software. Lane 1, Δ*pdr5;* lane 2, WT; lane 3, E1013A; lane 4; G312A. *B,* Quantitative analysis of clotrimazole resistance. Cultures containing drug were prepared as previously described (Sauna *et al*., 2008). The plots and statistical analyses were performed using GraphPad Prism software. The data points are the average of at least three independent experiments. *C,* Quantitative analysis of cycloheximide resistance. Cultures containing drug were prepared as previously described (Sauna *et al*., 2008). The plots and statistical analyses were performed using GraphPad Prism software. The data points are the average of at least three independent experiments. D, Rhodamine 6G efflux of WT and mutant strains was performed as previously described (Sauna *et al*., 2008). A representative plot is shown. Three independent determinations were made with each strain.

Drug phenotype of C199A is very similar to E1013A

In canonical ABC transporters and in other ATPases using the Walker A and B motifs, the Walker A region contains a completely conserved and essential lysine residue. In Pdr5, Ernst *et al*., (2008) reported that K911M is phenotypically null; an observation that was confirmed by our lab. In the Pdr5 family, however, the deviant ATP binding site has a completely conserved cysteine residue (Cys-199) in place of lysine. Interestingly, a lysine (AAA/G) to cysteine (T/UGC) substitution requires three genetic alterations. Ernst *et al*. (2008) reported that a C199A alteration had no effect on ATPase levels and resistance to several drugs including cyh, ketoconazole, and rhodamine 123. R6G efflux was unimpaired. In contrast to work with Pdr5, Jha *et al.*, (2003) studied the same mutation in Cdr1p (C193A) and concluded that it was required for ATP hydrolysis as 95% of the activity was lost.

In light of the results with E1013A, this issue in Pdr5 was reexamined. The C199A mutation was recreated and its resistance to clo and cyh was tested (Figure 10B, 10C). As reported by Ernst *et al*., (2008) K911M is phenotypically null on clo. The C199A mutation exhibits significant clo hypersensitivity when compared to WT. The reduction in resistance is similar to E1013A (Figure 10B). On cyh, C199A has a MIC of 5µM about 1.5 times less than WT. However C199A is 5 times more resistant than E1013A. The R6G transport data for C199A clearly shows that the deviant Walker A mutant retains considerable transport capability (Fig 1D). The median retained fluorescence for C199A is 5.78 which is very similar to WT (11.24). This result is consistent with Ernst *et al.,* (2008). The transport capability of the deviant Walker A mutant is similar to the deviant signature mutant E1013A, which further emphasizes the fact that the deviant ATP binding site plays an important role in protein function.

E1013A and C199A retains significant ATPase activity

The ATPase activity of the signature mutants (E1013A and G312A) and deviant Walker A mutant (C199A) were measured. The equivalent signature moif mutations and the deviant Walker A mutation C193A of Cdr1 resulted in a null phenotype with respect to drug resistance and ATPase activity (Kumar *et al.,* 2010). In Pdr5, however, the phenotypic assay of clo and cyh resistance and R6G transport, strongly suggested that the deviant signature residue E1013A and the deviant Walker A residue C199A retains significant ATPase function. The ATPase activity of the mutants was measured (Figure 11). The G312A mutation had no significant ATPase activity and was fully consistent

with its null or nearly null phenotype. In contrast, E1013A had reduced, but significant ATPase. The V_{max} of E1013A is about 50-60 nmol / min / mg which was about one-third of WT (~220 nmol/min/mg). The K_ms of E1013A and WT are indistinguishable. This suggests that E1013A and G312A are phenotypically very different and unlike G312A, E1013A may not be required for catalysis of ATP. Furthermore, like E1013A, the ATPase activity of C199A is about 25% of the WT. These results clearly indicate that, although, the deviant Walker A and signature residues, Cys-199 and Glu-1013 are not completely dispensable, they are clearly not required for catalytic action.

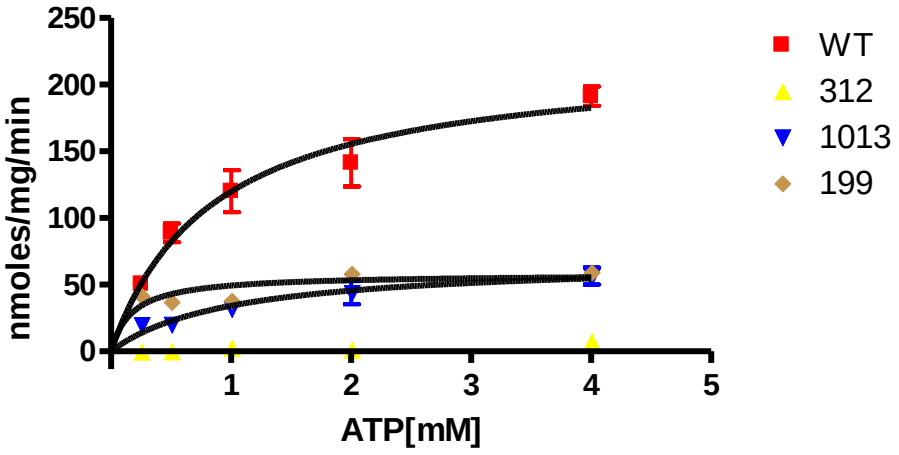

Figure 11: Pdr5 mediated ATPase activity in WT and mutant strains. The Pdr5-specific ATPase activity was measured as previously described (Sauna *et al*., 2008) in double-copy strains. 12 µg of PM vesicle protein was used in each reaction. The plots of activity versus ATP concentration were made and analyzed with Graph Pad Prism software. The data represent the average of three independent experiments and at least two independent batches of PM vesicles per strain.

The suppressors of E1013A lie outside PDR5

The isolation and characterization of mutations that suppress a mutant phenotype is a well-known classic genetic tool to identify interacting residues in a protein. This method has been previously employed to map a large part of the Pdr5 signal interface (Sauna *et al*., 2008). In order to isolate suppressors of G312A and E1013A cultures of these mutants were plated on 5 µM clo. The G312A mutation yielded no colonies in 9/10 cultures plated. A single culture plate yielded 7 colonies. When a dilution series was performed, the phenotype was indistinguishable from the WT strain. The PDR5 DNA was recovered from three of these cultures and sequenced. Each contained an A312G reversion. Thus, in this jackpot, the WT sequence was restored. This is entirely plausible as a single base-pair substitution can interchange these residues. Furthermore, the result is not entirely surprising as the conserved Gly in the signature motif is thought to play a specific role in anchoring the nucleotide and other residues in the vicinity probably can't substitute.

The results with the E1013A substitution were very different. Suppressor mutations of E1013A, in contrast were recovered at a relatively high frequency of about 0.5×10^{-5} on 5 µM clo. (Figure 12) contains a scan of a dilution series that clearly shows that although all of the suppressors are more resistant than E1013A, most are significantly more sensitive than WT. Two, however, were also more resistant than the wild type. DNA from eight independent suppressor mutations was obtained by PCR and

the *PDR5* coding region was completely sequenced. Although the original E1013A mutation was present, no additional alterations were observed. Two suppressors, #5 (SUP5) and #6 (SUP6) were analyzed further. Data in Figure 13 A demonstrate that when a quantitative IC_{50} is carried out with clo, the SUP6 suppressor is about two times more resistant than E1013A and SUP5 is phenotypically.

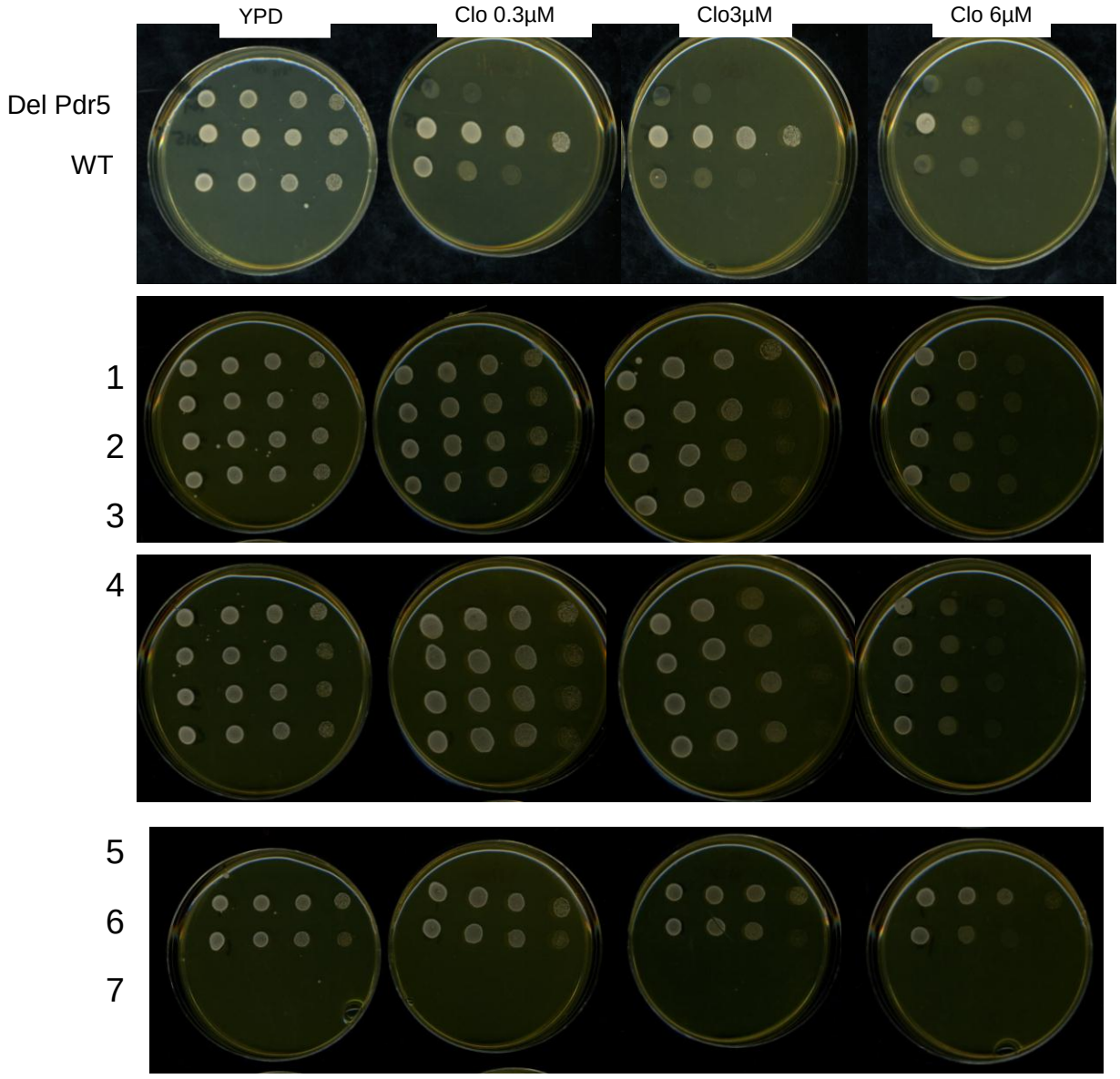

Figure 12. Intergenic suppressors of E1013A clotrimazole hypersensitivity-Spot test. A ten-fold dilution series spot test was performed. Four dilutions were made: 0.5 X 10^6, 0.5 X 10^5, 0.5 X 10^4 and 0.5 X 10^3. These were spotted in a volume of 5 µl on solid medium containing a fixed concentration of clo (1.5, 3.0, and 6.0 µM). The plates were incubated at 30°C for 96 hr before scanning

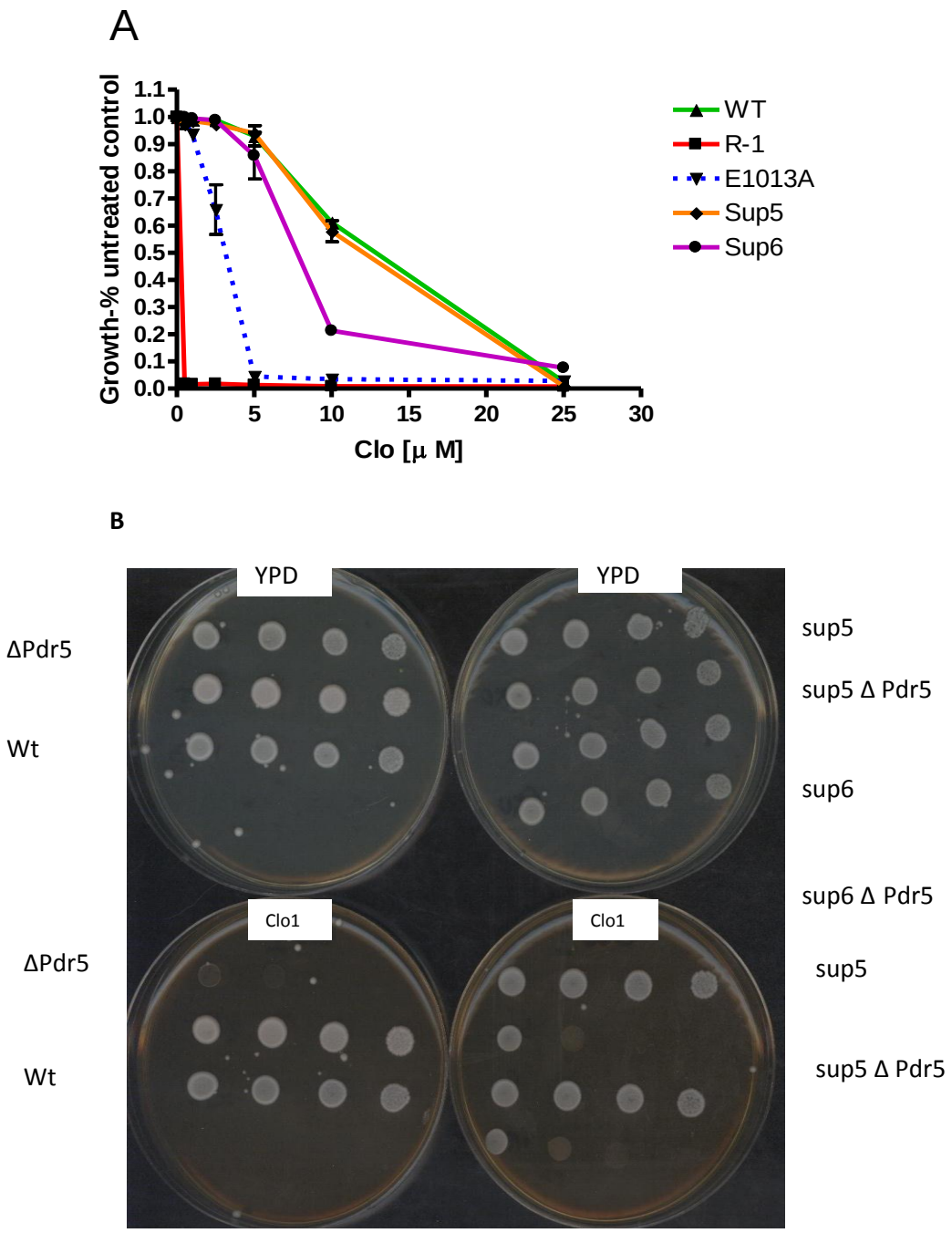

Figure 13. Intergenic suppressors of E1013A clotrimazole hypersensitivity-Quantitative analysis. *A,* Quantitative analysis of clo resistance was performed with SUP5 and SUP6. The plots represent the average of at least three independent experiments. *B,* The effect on the suppressors of eliminating Pdr5 was evaluated with a ten-fold dilution series spot test on clo plates ranging from 0.15 µM to 3.0 µM. Knock

outs were made in two steps. The KanMX4 cassette was recovered by PCR. This DNA was used to transform the SUP5 and SUP6 strains. Transformants were selected on G418 medium (formerly called geneticin medium). PCR was used to verify the presence of a knock out mutation.

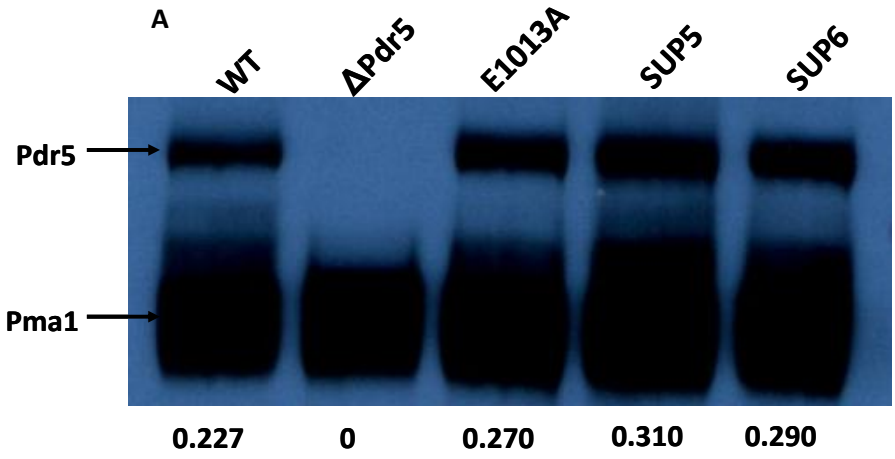

Figure14. Intergenic suppressors of E1013A clotrimazole hypersensitivity-Immunoblot. *A, I*mmunoblotting of PM vesicles from SUP5 and SUP6 was performed. The number in each lane is the ratio of Pdr5 to Pma1 and was determined using ImageJ software. Lane 1; Δ*pdr5*; lane 2, WT; lane 3, SUP5; lane 4; SUP6.

SUP5 and SUP6 localize in membrane at levels equivalent to WT

The easiest explanation for the suppressor effect is that these mutations occur in proteins that regulate the level of Pdr5 in the plasma membrane. Thus, genetic changes that raise the level of Pdr5 could raise the resistance of the E1013A mutation. In order to address this question, the steady-state PM level of Pdr5 in two suppressors was compared by western blotting to the level observed in the original E1013A mutation. These results

are found in Figure 14A demonstrate that there was no difference when the levels of Pdr5 are compared to those of Pma1 for each strain.

The suppressor phenotype requires Pdr5 protein

The inability to suppress a G312A mutant strongly suggests that most of the E1013A intergenic suppressors are interfacing with the deviant ATP-binding site and are not simply mutations in an independently functioning protein. To address this issue, the *pdr5::KanMX4* cassette from R-1 and used it to replace E1013A in the two suppressors, SUP5 and SUP6 under investigation. Thus, as a result of transformation this mutation was replaced with a complete deletion of Pdr5. The presence of the knockout mutation in the strains was verified by PCR. Following this, the relative clo resistance of SUP5Δpdr5 and SUP6 Δpdr5 was compared to E1013A, SUP5 and SUP6 along with positive and negative controls. These results are found in Figure 13 B where the strains in question are compared on several concentrations including 0.5 μM clo; a low dose of the drug that nevertheless kills the Δ*pdr5* strain. The results of a serial dilution spot test clearly demonstrate that the drug resistance observed with the suppressors is reduced to a level in both knockout strains that is nearly equivalent to *Δpdr5*. Therefore, as expected, the suppressor mutations require Pdr5 for clo resistance.

SUP5 restores ATPase activity to WT levels

Unlike the suppressors of the signal deficient mutation S558Y which restore significant transport without further increasing ATPase levels, the SUP5 mutation significantly improves ATPase activity (Figure 15). SUP 5 increases the ATPase activity back to WT levels. The V_{max} of SUP5 (137.20 nmol / min / mg) was very similar to WT levels (88.91 nmol / min / mg). However, it is interesting to note that Km of SUP6 is no different from E1013A (20 nmol / min / mg) even though SUP6 was twofold more resistant to clo than E103A.

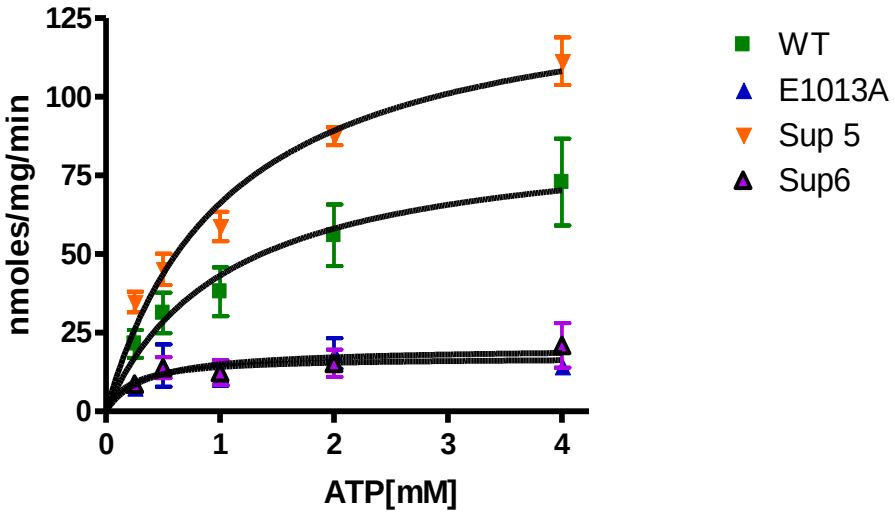

Figure 15: ATPase activity of SUP5 and SUP6. ATPase activity was assayed as previously described. In these experiments, all of the strains contained only a single copy of *PDR5* in contrast to double copy strains used in previous results. Thus, 16 µg of PM vesicle protein was used in each reaction.

Microarray analysis of SUP5

After the phenotypic characterization of SUP5, the next step was to identify the gene responsible for the SUP5 phenotype. Genetic analyses of SUP5 by Dr. Golin suggest that SUP5 has a dominant and unstable phenotype. Thus SUP5 strains throw off colonies with E1013A levels of sensitivity at a frequency of ~1.3%. Classically, intergenic suppression is caused by over expression of wildtype sequences. The purpose of the microarray analysis was to identify candidate targets responsible for the SUP5 phenotype which restores resistance of clo hypersensitive E1013A back to WT. 1 ml over night culture of SUP5, E1013A and an unstable segregant were outsourced to Array One (San Diego, CA) for microarray analysis. The expression level of 6000 yeast genes was measured in the three culture samples. The data was then analyzed by making a three way comparism between SUP5, E1013A and the unstable segregant. We posited that if the SUP5 phenotype is due to overexpression of a particular gene product, the expression level of the target would be 3-5 fold higher in SUP5 (S) than E1013A (E); however the expression in the unstable (U) segregant would be reduced to a level closer to E1013A. Initial data screening done by setting U/E expression ratio to >0 and S/E ratio to >1.5, revealed approximately 46 candidate genes products (Table 4). Interestingly, out of the 46 genes, 20 appeared as a cluster on the right arm of chromosome VIII. Therefore, the probability that the target gene of interest is located on chromosome VIII appears high. Smaller clusters were also present on chromosome XII and XIII. Chromosome loss experiments will be continued by Dr. Golin to identify the chromosome on which the

gene responsible for SUP5 phenotype is located. The chromosome walking techniques will be employed to locate the actual gene.

Table 3: Microarray Data

GENE NAME	CHROMOSOME	GENE DESCRIPTION
OCH_DS100_YAR064W	I	operon cross hyb
TS(AGA)A	I	tRNA
TLC1	II	noncoding rna
TT(AGU)B	II	tRNA
TF(GAA)D	IV	tRNA
AIR1	IX	RING finger protein
MIG3	V	Transcriptional repressor involved in response to toxic agents
YFR012W-A	VI	Putative protein of unknown function
GSC2	VII	Catalytic subunit of 1,3-beta-glucan synthase
OCH_YHR094C_HXT1	VIII	operon cross hyb
HXT1	VIII	Low-affinity MFS glucose transporter
YHL035C	VIII	Member of the ATP-binding cassette (ABC) family
DBP8	VIII	ATP-dependent RNA helicase of the DEAD-box family
BCD1	VIII	Protein required for the accumulation of box C/D snoRNA
SPO13	VIII	Meiosis-specific protein
YHR048W	VIII	Protein similar to MDR proteins
YHR214C-D	VIII	orfs not included in aros set
CIC1	VIII	Essential protein that interacts with proteasome components
SSF1	VIII	Constituent of 66S pre-ribosomal particles
ARO9	VIII	Aromatic aminotransferase
YHL037C	VIII	Hypothetical protein
OTU2	VIII	Member of the ovarian tumor-like (OTU) superfamily
IMD2	VIII	Inosine monophosphate dehydrogenase
RPF1	VIII	Nucleolar protein
MNL1	VIII	Alpha mannosidase-like protein of the ER

GENE NAME	CHROMOSOME	GENE DESCRIPTION
IMP3	VIII	Component of the SSU processome
REC104	VIII	Protein involved in early stages of meiotic recombination
IRE1	VIII	Serine-threonine kinase and endoribonuclease
YHR182W	VIII	Protein of unknown function
SCH9	VIII	Protein kinase that regulates signal transduction activity
PEX28	VIII	Peroxisomal integral membrane protein
UBA4	VIII	Protein that activates Urm1p before its conjugation to proteins
HXT8	X	Protein similar to hexose transporter family member
YJR114W	X	Protein involved in survival during stationary phase
BUD2	XI	GTPase activating factor for Rsr1p/Bud1p
RRN_JXN_25S_ETS2	XII	ribosomal RNA
YLRCTY2-2	XII	retrotransposon
RRN_ITS1-1	XII	ribosomal RNA
YMR265C	XIII	Hypothetical protein
YML034C-A	XIII	Hypothetical protein
MSS11	XIII	Transcription factor
PHO84	XIII	High-affinity inorganic phosphate (P_i) transporter
SNR49	XIV	snoRNA
YNL095C	XIV	Hypothetical protein
OCH_YOL156W_HXT11	XV	operon cross hyb
OCH_YOR192C-C_YOR192C-C	XV	operon cross hyb

DISCUSSION

The recently resolved structures of Sav1866 (Locher *et al.,* 2006) and crosslinking studies *(*Linton *et al.,* 2007 and Tampe *et al.,*2009)provide insights into the coupling interface of ABC proteins. The coupling of ATP hydrolysis (at the NBDs) to transport (at the TMDs) is one of the most critical steps of the transport cycle of ABC proteins. Characterizing the coupling interface in a functional protein, however, is challenging. We previously developed a genetic screen coupled with biochemical assays to identify residues associated with the coupling interface in the yeast ABC transporter Pdr5 (Golin *et al.,* 2008). In that study, we exploited a mutation at the extracellular end of TMH2 (S558Y). ATP hydrolysis and molecular movements in the TMHs (which bring about transport) are uncoupled in the mutant Pdr5, which shows both ATP hydrolysis and binding of the transport substrate, IAAP, but no drug resistance. Our strategy was to screen for second-site mutations that restore drug resistance, because these suppressors should identify interacting residues. We reported that the double-mutant S558Y, N242K exhibited almost a complete reversal of the null phenotype of S558Y. The location of N242K was consistent with the NBD face of the coupling interface surmised from the X-ray crystallographic structure of the bacterial ABC multidrug transporter Sav1866 (Locher *et al.,* 2006) as well as with crosslinking studies on P-glycoprotein (Linton *et al.,* 2007). In the current study we extended our work to further elucidate the coupling interface of Pdr5, identifying key residues in both the NBD face of the protein and ICL1, which connects TMHs 2 and 3.

We used the mutant S558Y to screen for clones that reverse the drug-sensitive phenotype of this mutant as described in detail previously (Golin *et al.,* 2008). Upon sequencing the Pdr5 gene in the revertants, we identified nine second-site mutations (including N242K from the previous study), representing 5 unique point mutations and one triplet-codon deletion. Four of these occurred in the NBD and were located almost contiguous to each other at positions 242, 244, and 246 (one independent mutant each of N242K and E244G and two independent mutants with D246del). The residue Glu-244 is equivalent to the conserved glutamine that is used to identify the Q-loop within the NBDs of ABC transporters. Thus, four of the nine second-site mutations appear to define the NBD face of the coupling interface and are proximal to or at the Q-loop. An additional 3 are in Ser-597, which is in the ICL1.The structure of Sav1866 suggested that conserved Q and X-loops might interact with the ICL1 to couple ATP hydrolysis to drug transport. The residues we identified lie in the same region of Pdr5. Moreover, the residue Glu-244 in Pdr5 lies at the same position as the conserved Q in other ABC transporters, and the glutamic acid at this position is completely conserved in the Pdr5 family.

Our results are consistent with the suggestion put forward by several authors that the Q-loop is implicated in intradomain coupling (van Veen *et al.,* 2009 and George *et al.,* 2004). Besides the second-site mutations in the NBD, we identified three additional point mutations in ICL1, and all were in the same residue, Ser-597. Thus, both faces of the interface—the NBD as well as the ICL—were recovered in our collection. Although ICL1 is predicted to be approximately 21 amino acids long, the identification of Ser-597 as a second-site mutant in three independently derived colonies suggests that relatively

few residues in this loop actually participate in critical contact with the ATP-binding sites.

The genetic screen therefore provides a functional confirmation of the suggestion prompted by the structure of Sav1866 that the NBDs interact with the TMDs via ICLs. This is found in all ABC transporters analyzed to date. However, the functional, genetic evidence from the current study suggests that the Pdr5 signaling interface is in the cis configuration—at least when transporting clo. The inferred pathway is N-terminal NBD Q-loop region (Asn-242, Glu-244, and Asp-246) to ICL-1 (Ser-597) to TMD1 (Ser-558, Met-679). An atomic model of Pdr5 shows that E244 lies very close to ICL1, but it is also directly under ICL4, which connects TMH 10 and 11 in TMD2 (R. Rutledge, unpublished observations). Thus, a trans configuration is also theoretically feasible. However, we did not recover any NBD2 (trans) suppressors of S558Y, but we found 4 independent mutations in NBD1. Similar results were obtained by selecting cyh^r suppressors of N242K in NBD1. It remains to be seen whether the trans configuration is ever used physiologically. An interesting future experiment would be to determine whether selection of S558Y suppressors on other Pdr5 transport substrates leads to second-site mutations in NBD2.

Two possible explanations are strongly implied by these findings. Pdr5 may differ from all prokaryotic and eukaryotic ABC efflux pumps analyzed to date. Structural studies of several importers, however, such as *E. coli* ButCD, which influxes vitamin B, and ModBC, which is an archeamolybdate pump, appear to have a signal interface in the cis configuration *(*Rees *et al., 2002* and Locher *et al., 2007).* Because Pdr5 is evolutionarily distant from these, it would be important to determine whether other eukaryotic members

of the ABC family have this arrangement. Other studies were conducted in the absence of transport substrate, whereas our mutants were selected on drug plates, so it is also quite possible that both cis and trans exist physiologically. For instance, it is plausible that drug binding results in conformational switching.

The Walker A and Walker B domains of the N-terminal NBD and the signature region of the second NBD vary significantly in the identity of key conserved residues vis-à-vis other ABC transporters. Thus, together they make up a deviant ATP-binding site. Because Glu-244 replaces the canonical Gln in the Q-loop, we characterized it in an otherwise WT background as well as the equivalent Gln-951 in NBD2.

The effect of site-directed mutagenesis on Q-loop residues was studied in mouse P-gp by Urbatsch *et al.,* 2000. In mouse P-gp, these residues are Gln-471 and Gln-1114 in the NBD1 and 2, respectively. The mutants Gln-471A and Gln-1114A showed a reduction in ATPase activity. However, in no case was the impairment greater than two orders of magnitude, and the K_m (ATP) was not altered, leading the authors to conclude that the mutations had no major effect on the substrate binding or on reaction chemistry *(*Urbatsch *et al., 2000)*. Furthermore, mutations in either of the two P-gp catalytic sites produced the same effects, implying functional symmetry.

Because the most obvious effect of the Gln-471A or Gln-1114A mutation was to reduce stimulation of ATPase activity by transport substrates, it was hypothesized that such residues play a critical role in interdomain communication. Mutations in either the Glu-244 or Gln-951 residue of Pdr5 had similar effects on ATP hydrolysis (Figure 6); although ATP hydrolysis was diminished, a significant residual activity remained, and the K_m was unaffected. We also studied E244G, Q951G, which showed no less ATPase

activity than that, observed in either of the two single mutants (Figure 6B). GTPase activity, which our previous work suggests has a physiological role to play in Pdr5-mediated transport, decreased even less than ATPase activity. Thus, our data are consistent with these residues being nonessential to the reaction chemistry (such as activation of the attacking water for ATP hydrolysis). However, unlike the K_m of ATP hydrolysis, the IC_{50} for the Pdr5 transport substrates clo and cyh is significantly decreased in both the E244G and Q951G mutant. Moreover, Pdr5-mediated drug resistance is largely abrogated in the double mutant, E244G, Q951G. Its phenotype is almost equivalent to the S558Y strain originally used to isolate the suppressor collection. It was evident that the reduced resistance to drug substrates in the E244G, Q951G double mutant was not a consequence of impaired binding of the transport substrate. E244G was initially isolated as a suppressor of the faulty-signaling S558Y mutant, and the results from the current study further indicate that the primary role of the conserved residues Glu-244 and Gln-951 is to communicate signals from the ATP sites to the TMDs via the ICLs. Furthermore, the much greater drug sensitivity of the double mutant and the similarity in phenotype of the single mutants strongly implies that these residues are functionally overlapping even though one is from a deviant portion of NBD-1. Equivalence of function is, of course, a striking feature of symmetric transporters such as P-gp; hence the phenotypic similarity of the Q-loop residue mutants (Q471A and Q1114A). Asymmetric transporters may differ, however. For instance, mutation of the conserved Walker A lysine in Tap1 and the analogous residue in Tap2 (Tap1 and Tap2 make up a peptide-translocating heterodimer) results in different effects on ATP binding and peptide transport *(*Lapinski *et al.*, 2001 and Hollenstein *et al.*, 2007). A similar

nonequivalence is observed in MRP1. Mutation of the same residue in the Walker A motif of each NBD has disparate effects on nucleotide binding (Hollenstein *et al.,* 2007).The observation, therefore, that the Q-loops of Pdr5 are equivalent and overlapping strongly implies that both ATP-binding sites are sending signals to the TMDs.

Pdr5 has a high basal ATPase that is not stimulated further by the addition of exogenous transport substrates (Balzi *et al.,* 1994). In this regard, it is strikingly different from P-gp. Our data also strongly suggest that Pdr5 is not especially efficient at coupling ATP hydrolysis to transport and they support the contention that much of this activity is uncoupled (Ernst *et al.,* 2010). For instance, although the S558Y, E244G and S558Y, N242K suppressors restore cyh resistance 8-fold, they show no restoration of ATPase activity. We speculate that WT ATPase is required for WT drug efflux. However significant transport can be achieved with much less ATPase activity. The reduced ATPase activity possibly reflects a loss of proper alignment of residues in the ATP binding site because of the mutations. The Pdr5 family of fungal transporters appears distinct from all other eukaryotes and may be a unique, but clinically important evolutionary variant.

In the first part of this study, suppressors of S558Ywere isolated to understand the interdomain communication between the TMD's and NBD's. The second site suppressors recovered were present in TMD1, ICL1 and NBD1, suggesting a signal interface pathway running from the N-terminal NBD (NBD1) via the Q loop region (Asn-242, Glu-244, Asp-246) and ICL1 (Ser-596) to TMD1 (Ser-558, Met-679). A large majority of suppressors were located in the N-terminal NBD, which contains several

motifs that form the deviant ATP binding site. Therefore, the location of the suppressors suggests that the deviant ATP binding site plays an important role in Pdr5 function.

The goal of the second part of this study was to identify the role of the deviant ATP binding site. Numerous studies have revealed that both the canonical and the deviant sites are required for the functional activity of the protein. However, very little is known about the precise function of the deviant site. In order to understand the role of the deviant ATP binding site in Pdr5, the contribution of the deviant Walker A (C199) and a residue in the deviant signature motif (E1013) were evaluated for their ability to transport drugs and hydrolyze ATP.

The liquid MIC data demonstrates that these mutants fall into two discrete groups with distinct drug phenotypes. The canonical Walker-A (K911M) and the canonical signature (G321A) mutations are as severely clo and cyh sensitive as the isogenic Δpdr5 strain and therefore phenotypically null. Ernst *et al*., (2008) also observed that K911M was null in Pdr5. Biochemical analysis of the canonical signature residue (G305) in Cdr1 revealed that a small change (G→A) completely abolished drug transport (Kumar *et al*., 2010). These results indicate that the residues of the canonical ATP binding site are necessary for drug efflux. Thus, all 3 laboratories arrived at the same unsurprising conclusion.

In contrast we observed that the deviant ATP binding site mutants (Walker A-C199A and signature-E1013A) retain partial resistance. C199A exhibited clo hypersensitivity that was very similar to E1013A. Interestingly, on cyh, E1013A was much more sensitive than C199A. We speculate, that since the chemical properties of cyh is very different from clo, the mechanism by which they are effluxed out by Pdr5 may be

slightly different in each case. Cyh efflux may require the involvement of the deviant signature motif and the E1013A mutation may disrupt this contribution leading to cyh sensitivity. In contrast to the work with Pdr5, Glu-1004 is required for protein function in Cdr1 (Kumar *et al.,* 2010). Kumar *et al*., 2010 showed that mutating the glutamate at the fourth position in the deviant signature motif (LNVEQ) to alanine (E1004A) or an equivposition swapping of the deviant residue with canonical residue (E1004G) severely impairs transport. In contrast, our data demonstrate that mutations in the deviant Walker-A and signature regions retain significant drug transport. This result highlights the functional difference between the canonical and the deviant Pdr5 ATP binding site and is at variance with the Cdr1 work.

In parallel with the clo and cyh IC-50 studies, the transport capability of the mutants was also measured. The R6G results further emphasize the functional nonequivalance between the two ATP binding sites as mutations in the canonical sites (K911M and G312A) completely abolish transport whereas the deviant ATP binding site mutations (C199A and E1013A) retain considerable transport capability. Ernst *et al*., (2008) also tested the effect of a C199A mutation on ATPase activity, cyh resistance and R6G transport. They reported that the behavior of this mutation was equivalent to WT. Thus, their transport data is in complete agreement with ours, but we observed a reduction in ATPase activity.

The role of the deviant ATP binding site in Pdr5 remains controversial. Moreover it is unknown if the deviant site is even able to bind/hydrolyze ATP. The ATPase assay of the mutants led to the following observations. First, the canonical Walker-A (K911) and signature (G312) residues play important roles and are required for catalysis of ATP as

the K911M and G312A mutation completely abolish ATPase activity. This result is consistent with the observations made earlier (Ernst *et al*., 2008). Mutation in the Cdr1 canonical signature, G305A, eliminates ATPase activity (Kumar *et al.,* 2010). Their model posits that the alanine mutation cause steric hindrance and thus obstructs function. Structural studies with Sav1866 suggest that the signature motif acts as a sensor for the ATP molecule interacting with Walker-A in the opposite NDB (Dawson *et al.,* 2006).

Second, the deviant Walker-A (C199A) and signature (E1013A) mutants retain significant ATPase activity, indicating that these residues are not required for catalysis. Also, the amount of ATP hydrolyzed by C199A is very similar to E1013A. However, in sharp contrast with our work, Kumar *et al.,* (2010) reported that the deviant signature mutation in Cdr1 (E1004A and E1004G) had no ATPase activity indicating their catalytic involvement in ATP hydrolysis (Kumar *et al.,* 2010). The same group also investigated the role of Cdr1 deviant Walker A (C193). They reported that a C193A mutation completely abolishes drug transport and ATPase activity suggesting that the Cdr1 deviant Walker A is critical for ATPase activity (Shukla *et al.,* 2006). Given the very high homology between Cdr1 and Pdr5, it is hard to believe the differences in mutant behavior can be due to different biochemical mechanisms. The Cdr1 deviant Walker A and deviant signature conclusions were drawn from biochemical studies with the purified N-terminal NBD which might not be physiologically relevant as the NBD's form a hybrid dimer in a head-to-tail fashion sandwiching one ATP molecule in between; whereas our work was done with intact protein which should make our results physiologically relevant. Furthermore it should be pointed out that the single NBD ATPase activity is only 10% of that observed with the intact Cdr1 transporter.

Based on the phenotype of the Pdr5 mutants it can be speculated that though the deviant site is not involved in catalysis, it is not completely indispensable. We propose that the deviant site may play a role in assisting the canonical site to perform its function. The deviant site could also promote or aid the binding/hydrolysis of ATP at the canonical site or play a regulatory role.

Since both the single deviant ATP binding site mutants C199A and E1013A retained partial drug resistance and ATPase phenotype, we posited that making a double mutant C199A, E1013A might give a null phenotype. However to our surprise, the double mutant did not localize to the membrane. It is interesting to note that residues located in the NBD and that are part of the deviant ATP binding site could affect membrane localization. A similar observation was made with L183P mutation located in the Walker A motif (Ghislain *et al*., 2007). This result further emphasizes the point that the deviant ATP binding site is not dispensable and plays an important role in Pdr5 function.

To further decipher the role of the deviant ATP binding site, we attempted to isolate intragenic suppressors of deviant signature (E1013A) and canonical signature (G312A) mutants. As suppressor isolation is a well-known way to identify interacting residues, it was thought that, if the deviant signature site is interacting and functioning along with the deviant Walker A, Walker B and Q-loop in the opposite NBD, then suppressors in the opposite NBD might be recovered. This would indicate the formation of a functional deviant ATP site. The suppressor screen yielded interesting results. No suppressors were recovered for G312A. This result further emphasizes the fact that Gly present at the fourth position in the canonical site is critical for ATP binding/catalysis and no other

residue in its vicinity can take over the function of G312. On the other hand, the E1013A mutation yielded ten suppressors. Surprisingly, all the second site suppressors were intergenic. Further investigation revealed that Pdr5 is required for suppressor action and the suppressor phenotype is not caused by Pdr5 over expression. This indicates that the suppressor protein is acting along with Pdr5 to alter Pdr5 structure/function. Suppressor 5 (Sup5) and suppressor 6 (Sup6) were analyzed further in this study. Biochemical analysis revealed that Sup5 and Sup6 were phenotypically different. Sup5 was able to restore ATPase activity and drug resistance back to WT. Sup6, however, restores partial resistance but has no effect on ATPase activity. Therefore, our model suggests that Sup5 and Sup6 might restore resistance to E1013A by separate mechanisms.

The phenotype of Sup6 is similar to signal interface mutants (E244G, Q951G) that improve resistance but have no effect on ATP hydrolysis (Ananthaswamy *et al.*, 2010). Therefore it can be suggested that Sup6 is improving the transmission interface of Pdr5, thereby improving efflux without having an effect on the amount of ATPase activity. Sup5 on the other hand, restores both drug resistance and ATP hydrolysis to WT levels, suggesting that there is an overall improvement in pump function. This result is also consistent with the observation that E1013A is not catalytic as the mutant does not preclude WT function in the presence of the intragenic suppressor. Based on our results we propose a model for Sup5 function.

The CFTR chloride channel has a built in regulatory domain (R-region) near NBD1 in the cytosol. This R-region is made up of approximately 200 residues and contains PKA phosporylation sites (King *et al*., 2009). The R-region plays an important role in regulating channel activity and fine tuning pump function. (Baker *et al.*, 2007). Forman *et*

al., (2007) showed that the unphosphorylated R-region acts a negative regulator by binding NBD1. Phosphorylation of the R-region results in dissociation from the NBD1, thereby allowing for ATP hydrolysis (Hanrahan *et al.,* 2005). Pdr5 does not have an obvious built in regulatory domain. Also, there are no known regulators of Pdr5 activity. However, it can be hypothesized that Sup5 is a novel cytosolic protein functioning as a regulator of Pdr5 that interacts with the deviant ATP binding site modulating ATPase activity. The data suggest that Sup5 is physiologically relevant in modulating Pdr5 function. Further biochemical analysis of the suppressors of E1013A will shed more light on the role of the deviant ATP binding site in Pdr5.

REFERENCES

Ananthaswamy, N., Rutledge, R., Sauna, Z. E., Ambudkar, S. V., Dine, E., Nelson, E., Xia, D., and Golin, J. 2010. The Signaling Interface of the Yeast Multidrug Transporter Pdr5 Adopts a Cis Conformation, and There Are Functional Overlap and Equivalence of the Deviant and Canonical Q-Loop Residues. *Biochemistry.* 49: 4440–4449.

Ambudkar, S. V. 1998. Drug-stimulatable ATPase activity in crude membranes of human MDR1-transfected mammalian cells. *Methods. Enzymol.* 292: 504-514.

Ambudkar, S. V., Lelong, I. H., Zhang, J., Cardarelli, C. O., Gottesman, M. M., and Pastan, I. 1992. Partial purification and reconstitution of the human multidrug-resistance pump: characterization of the drug-stimulatable ATP hydrolysis. *Proc. Natl. Acad. Sci. U. S. A.* 89: 8472–8476.

Balzi, E., Wang, M, Leterme, S., Dyck, L. V., and Goffeau, A. 1994. PDR5, a novel yeast multidrug resistance conferring transporter controlled by the transcription regulator PDR1. *J. Biol. Chem*. 269, 2206–2214.

Boeke, J. D., Trueheart, J., Natsoulis, G., and Fink, G. R. 1987. 5-Fluoroorotic acid as a selective agent in yeast molecular genetics. *Methods Enzymol.* 154: 164–175.

Davis, J. E., Voisine, C., and Craig, E. A., 1999. Intragenic suppressors of Hsp70 mutants: Interplay between the ATPase- and peptide-binding domains Proc. *Natl. Acad. Sci. U. S. A.* 96: 9269–9276.

Dalmas, O., Orelle, C., Foucher, A. E., Geourjon, C., Crouzy, S., Pietro, A. D., and Jault, J.M. 2005, The Q-loop disengages from the first intracellular loop during the catalytic cycle of the multidrug ABC transporter BmrA. *J. Biol. Chem*. 280: 36857–36864.

Dawson, R. J., and Locher, K. P. 2006. Structure of a bacterial multidrug ABC transporter. *Nature* 443: 180–185.

Decottignies, A., Kolaczkowski, M., Balzi, E., and Goffeau, A. 1994. Solubilization and characterization of the overexpressed PDR5 multidrug resistance nucleotide triphosphatase of yeast. *J. Biol. Chem*. 269: 12797–12803.

de Thozee, C. P., Cronin, S., Goj, A., Golin, J., and Ghislain, M., 2007. Subcellular trafficking of the yeast plasma membrane ABC transporter, Pdr5, is impaired by a mutation in the N terminal nucleotide binding fold. *Mol. Microbiol.* 63: 811–825.

Ernst, R., Kueppers, P., Klein, C. M., Schwarzmueller, T., Kuchler, K., and Schmitt, L. 2008. Amutation of the H-loop selectively affects rhodamine transport by the yeast multidrug ABC transporter Pdr5.*Proc. Natl. Acad. Sci. U. S. A.* 105: 5069–5074.

Ernst, R., Kueppers, P., Stindt, J., Kuchler, K., and Schmitt, L., 2010. Multidrug efflux pumps: Substrate selection in ATP-binding cassette multidrug efflux pumps;first come, first served. *FEBS J.* 277: 540–549.

Golin, J., Ambudkar, S., Gottesman, M., Habib, A., Sczepanski, J., Ziccardi, W., and May, L., 2003. Studies with novel Pdr5p substrates demonstrate a strong size dependence for xenobiotic efflux. *J. Biol. Chem*. 278: 5963–5969.

Golin, J., Kon, Z. N., Wu, C. P., Martello, J., Hanson, L., Supernavage, S., Ambudkar, S. V., and Sauna, Z. E., 2007. Complete inhibition of the Pdr5p multidrug efflux pump ATPase by its transport substrate clotrimazole suggests that GTP as well as ATP may be used as an energy source. *Biochemistry* 46: 13109–13119.

Golin, J., Ambudkar, S. V., and May, L., 2007. The yeast Pdr5p multidrug transporter: How does it recognize so many substrates? *Biochem. Biophys. Res. Commun.* 356: 1–5.

Haimeur, A., Conseil, G., Deeley, R. G., and Cole, S. P. C. 2004. The MRP-related and BCRP/ABCG2 multidrug resistance proteins: biology, substrate specificity and regulation. Curr. Drug Metab. 5, 21–53.

Hanson, L., May, L., Tuma, P., Keeven, J., Mehl, P., Ferenz, M., Ambudkar, S. V., and Golin, J. 2005. The role of hydrogen bond acceptor groups in the interaction of substrates with Pdr5p, a major yeast drug transporter. *Biochemistry* 44: 9703–9713.

Higgins, C. F., and Linton, K. J., 2004. The ATP switch model for ABC transporters. *Nature* 11: 918 – 926.

Hollenstein, K., Frei, D. C., and Locher, K. P. 2007. Structure of an ABC transporter in complex with its binding protein. *Nature* 446: 213–216.

Jha S., Karnani N., Dhar S. K., Mukhopadhayay K., Shukla S., Saini P., Mukhopadhayay G., Prasad R., 2003. Purification and characterization of the N-terminal nucleotide binding domain of an ABC drug transporter of Candida albicans: uncommon cysteine 193 of Walker A is critical for ATP hydrolysis. *Biochemistry.* 36:10822-10832.

Jones, P. M., and George, A. M., 2004. The ABC transporter structure and echanism: Perspectives on recent research. *Cell. Mol. Life Sci*. 61:682–699.

Katzmann, D. J., Hallstrom, T. C., Voet, M., Wysock, W., Golin, J., Volckaert,G., and Moye-rowley, W. S., 1995. Expression of an ATP-binding cassette transporter-encoding gene (YOR1) is required for oligomycin resistance in Saccharomyces cerevisiae. *Mol. Cell. Biol.* 15: 6875–6883.

Kim, I.-W., Peng, X.-H., Sauna, Z. E., FitzGerald, P. C., Xia, D., Muller, M., Nandigama, K., and Ambudkar, S., V. 2006. The conserved tyrosine residues 401 and 1044 in the ATP sites of human P-glycoprotein are critical for ATP binding and hydrolysis: Evidence for a conserved subdomain, the A-loop in the ATP-binding cassette. *Biochemistry* 45: 7605–7616.

Kolaczkowski, M., van der Rest, M., Cybularz Kolaczkowska, A., Soumillion, J. P., Konings, W. N., and Goffeau, A., 1996. Anticancer peptides and steroids as substrates of the yeast multidrug transporter Pdr5p. *J. Biol. Chem.* 271: 31543–31548.

Kumar, A, Shukla, S, Mandal, A, Shukla, S, Ambudkar S. V., Prasad R., 2010. Divergent signature motifs of nucleotide binding domains of ABC multidrug transporter, CaCdr1p of pathogenic Candida albicans, are functionally asymmetric and noninterchangeable. *Biochimica et biophysica acta*. 1798:1757-66.

Lapinski, P. E., Neubig, R., and Raghavan, M., 2001. Walker A lysine mutations of Tap1 and Tap2 interfere with peptide translocation, but not peptide binding. *J. Biol. Chem.* 276: 7526– 7533.

Leonard, P. J., Rathod, P. K., and Golin, J. 1994. Loss of function mutation in the yeast multiple drug resistance gene PDR5 causes a reduction in chloramphenicol efflux. *Antimicrob. Agents Chemother*. 38: 2492–2494.

Linton K.J., 2007. Structure and function of ABC transporters. *Physiology*. 22:122-30

Lockless, S. W., and Ranganathan, R., 1999. Evolutionarily Conserved Pathways of Energetic Connectivity in Protein Families. *Science* 286: 295–299.

Locher, K. P., Lee, A. T., and Rees, D. C., 2002. The E. coli ButCD structure: A framework for ABC transporter architecture and mechanism. *Science* 296: 1091–1098.

Meyers, S., Schauer, W., Balzi, E., Wagner, M., Goffeau, A., and Golin, J., 1992. Interaction of the yeast pleiotropic drug resistance genes PDR1 and PDR5. *Curr. Genet.* 21: 431–436.

Monk, B. C., and Goffeau, A., 2008. Outwitting Multidrug Resistance to Antifungals *Science* 321, 367–369

Nakamura, K., Niimi, M., Niimi, K., Holmes, A. R., Yates, J. E., Decottignies, A., Monk, B. C., Goffeau, A., and Cannon, R. D., 2001. *Antimicrob. Agents Chemother.* 45: 3366–3374.

Neher, E., 1994. How frequent are correlated changes in families of protein sequences? Proc. *Natl. Acad. Sci. U. S. A.* 91: 98–102.

Oancea, G., O'Mara, M. L., Drew-Bennett, W F., Tielman, P., Abeles, R., and Tampe, R., 2009. Structural arrangement of the transmission interface in the antigen ABC transport complex TAP. *Proc. Natl. Acad. Sci. U.S.A.* 106: 5551–5556.

Pagant, S., Brovman, E.Y., Halliday, J.J. and Miller, E.A., 2008. Mapping of interdomain interfaces required for the functional architecture of Yor1p, a eukaryotic ATP-binding cassette (ABC) transporter. *J. Biol. Chem.* 39:26444-26451.

Paumi, C. M., Chuk, M., Snider, J., Stagljar, I., Michaelis, S., 2009. ABC Transporters in Saccharomyces cerevisiae and Their Interactors: New Technology Advances the Biology of the ABCC (MRP) Subfamily. *Microbiol. Mol. Biol.* 73:577-593.

Posteraro, B., Sanguinetti, M., Sanglard, D., La Sorda, M., Boccia, S., Romano,L., Morace, G., and Fadda, G., 2003. Identification and characterization of a *Cryptococcus neoformans* ATP binding cassette (ABC) transporter-encoding gene, *CnAFR1*, involved in the resistance to fluconazole. *Mol. Microbiol*. 47: 357–371.

Rai, V., Gaur, M., Kumar, A., Shukla, S., Komath, S. S., and Prasad, R., 2008. A novel catalytic mechanism for ATP hydrolysis employed by the N-terminal nucleotide-binding domain of Cdr1p, a multidrug ABC transporter of Candida albicans. *Biochem. Biophys. Acta* 1778, 2143–2153.

Riordan, J. R., 2008. CFTR function and prospects for therapy. *Annu. Rev. Biochem.* 77, 701–726.

Rogers, B., Decottignies, A.,Kolaczkowski, M., Carvajal, E., Balzi, E.and Goffeau, A., 2001. The pleiotropic drug ABC transporters from Saccharomyces cerevisiae. J. Mol. Microbiol. *Biotechnol.* 3: 207–214.

Rutledge, R. M., Ghislain, M., Mullins, J. M., de Thoz_ee, C. P., and Golin, J., 2008. Pdr5-mediated multidrug resistance requires the CPY-vacuolar sorting protein Vps3: Are xenobiotic compounds routed from the vacuole to plasma membrane transporters for efflux? *Mol. Genet. Genomics* 279: 573–583.

Rutledge, R., Esser, L., Ma, J., and Xia, D., 2011. Toward understanding the mechanism of the yeast multidrug resistance transporter Pdr5p: A molecular modeling study. *J Str Biol.* 173: 333–344

Sauna, Z. E., Nandigama, K., and Ambudkar, S. V., 2006. Exploiting reaction intermediates of the ATPase reaction to elucidate the mechanism of transport by P-glycoprotein (ABCB1). *J. Biol. Chem.*281: 26501–26511.

Sauna, Z. E., Bohn, S. S., Rutledge, R., Dougherty, M, P., Cronin, S., May, L., Xia, D., Ambudkar, S. V., and Golin, J., 2008. Mutations define cross-talk between the N-terminal nucleotide-binding domain and transmembrane helix-2 of the yeast multidrug transporter Pdr5. *J. Biol. Chem*. 283: 35010–35022.

Sauna, Z. E., and Ambudkar, S. V., 2007. About a switch: how P-glycoprotein (ABCB1) harnesses the energy of ATP binding and hydrolysis to do mechanical work. *Mol. Cancer Ther*. 6: 13–23.

Schumacher, M. A., Miller, M. C., Grkovic, S., Brown, M. H., Skurray, R. A., and Brennan, R. G., 2002. Structural basis for cooperative DNA binding by two dimers of the multidrug-binding protein QacR *EMBO J.* 21: 1210–1218.

Schumacher, M. A., and Brennan, R. G., 2003. Deciphering the molecular basis of multidrug recognition: crystal structures of the Staphylococcus aureus multidrug binding transcription regulator QacR. *Res. Microbiol*. 154: 69–77.

Schumacher, M. A., Miller, M. C., and Brennan, R. G., 2004. Structural mechanism of the simultaneous binding of two drugs to a multidrug-binding protein. *EMBO J*. 23: 2923–2930.

Seeger, M. A., and van Veen, H. W., 2009. Molecular basis of multidrug transport by ABC transporters. *Biochim. Biophys. Acta* 1794: 725–737.

Shukla, S., Saini, P., Smriti, Jha, S., Ambudkar, S. V., and Prasad, R., 2003. Functional characterization of *Candida albicans* ABC transporter Cdr1p *Eukaryot. Cell* 2: 1361–1375

Shukla, S., Rai, V., Banerjee, D., and Prasad, R., 2006. Characterization of Cdr1p, a major multidrug efflux protein of Candida albicans: purified protein is amenable to intrinsic fluorescence analysis *Biochemistry* 45: 2425–2435.

Urbatsch, I. L., Gimi, K., Wilke-Mounts, S., and Senior, A. E., 2000. Investigation of the role of glutamine-471 and glutamine-1114 in the two catalytic sites of P-glycoprotein. *Biochemistry* 39: 11921–11927.

Velamakanni, S., Yao, Y., Gutmann, D. A. P., and van Veen, H. W., 2008., Multidrug transport by the ABC transporter Sav1866 from *Staphylococcus aureus*. *Biochemistry* 47: 9300–9308

White, T. C., Marr, K. A., and Bowden, R. A., 1998., Clinical, cellular, and molecular factors that contribute to antifungal drug resistance. *Clin. Microbiol. Rev*. 11: 382–396.

Zolnerciks, J. K., Wooding, C, and Linton, K. J., 2007. Evidence for a Sav1866-like architecture for the human multidrug transporter P-glycoprotein. *FASEB J*. 21: 3937–3948.